T-AM-SymII-1 READING BETWEEN THE LINES IN THE STRUCTURE DATA BASE: TOWARD PRINCIPLES FOR NEGATIVE DESIGN. Jane S. Richardson and David C. Richardson (Duke University).
One of the major difficulties faced either by native proteins folding up to form a distinct tertiary structure, or by scientists in trying to predict such a structure or design a new one, is simply the fact that there are far too many plausible alternatives. An amino-acid sequence that is destined to form a soluble 4-helix bundle protein must of course prefer α-helical to extended β conformation; however, it must also avoid inserting into a membrane, starting with a strong signal sequence, dimerizing as a coiled-coil, binding an ion that stabilizes it in the wrong conformation, or assembling its helix bundle clockwise when it was supposed to be counterclockwise. We will describe some cases for which one can find evidence of such negative constraints from patterns of what does not occur in the known protein structures, and show how we try to apply such ideas in the *de novo* design of novel small proteins for synthesis.

T-AM-SymII-2 MOLECULAR STRUCTURE OF INSECTICYANIN AT 2.0 Å RESOLUTION
H.M. HOLDEN, J.H. LAW AND I. RAYMENT

Insecticyanin is a blue biliprotein found in the hemolymph and integument of the tobacco hornworm Manduca sexta L. and in conjunction with the yellow carotenoids, plays an integral role in the camouflage coloration of the insect. The chromophore reponsible for giving insecticyanin its intense blue coloration is the γ-isomer of biliverdin IX.

We have solved and refined the molecular structure of insecticyanin to a nominal resolution of 2.0 Å. The electron density map clearly demonstrates that the protein packs in the crystalline lattice as a tetramer with 222 symmetry. Each subunit has overall dimensions of 44 Å x 37 Å x 40 Å and consists primarily of an eight stranded anti-parallel β-barrel flanked on one side by a 4.5-turn α-helix. The biliverdin chromophore lies towards the open end of the β-barrel with its two propionate side chains pointing towards the solvent and it adopts a rather folded conformation much like a heme.

Interestingly the overall molecular fold of the insecticyanin subunit shows remarkable similarity to structural motifs observed in bovine β-lactoglobulin, human serum retinol-binding protein and rat intestinal fatty acid binding protein. Indeed, it may be that the three-dimensional architecture exhibited by these proteins is ideally suited for the effective binding and transport of hydrophobic and conjugated ligands.

T-AM-SymII-3 THE 1.9Å CRYSTAL STRUCTURE OF THE trp REPRESSOR/OPERATOR COMPLEX. Paul B. Sigler, Department of Biochemistry and Molecular Biology, University of Chicago, Chicago, IL.

The refined high resolution crystal structures of unliganded trp aporepressor, liganded trp repressor, falsely liganded trp pseudorepressor and the trp repressor/operator complex indicate the basis for a ligand-activated specific protein/DNA interaction. The protein contributes 28 direct hydrogen bonds to the operator, all but four are to the nonesterified phosphate oxygens. There are no direct hydrogen bonds or non-polar contacts with the bases that explain specificity. There are five water-mediated hydrogen-bonded systems, two involving phosphates and three involving three of the operator's most genetically sensitive base pairs. There is an unusually large (2900Å^2) solvent-excluded contact surface.

The orientation of the helix-turn-helix of the repressor in the crystalline complex deviates significantly from that of the free protein. The operator is segmentally bent and shows the largest local deviations from helically uniform DNA in the segment that is most sensitive to mutation. The normally mobile side chains on the repressor's surface are well fixed in the interface with the operator. Thus, both the protein and DNA adjust their conformations and "mesh" to form a highly stable interface. Specificity apparently arises through a combination of water-mediated hydrogen bonds to the critical bases and a base-sequence dependent effect that permits the operator (at a minimum cost in internal energy) to assume a conformation that forms this large, and especially stable interface.

T-AM-SymII-4 SOLUTION STRUCTURE OF SYNTHETIC "ZINC FINGER" DNA-BINDING DOMAINS.
G. Parraga, S. Horvath, L. Hood, E. T. Young, and R. E. Klevit, Dept. of Biochemistry, University of Washington, Seattle, WA and Dept. of Biology, CAL Tech., Pasadena, CA.

A novel DNA-binding motif that has come to be known as a "zinc finger" has been identified in a wide variety of eukaryotic proteins. A zinc finger consists of 30 amino acid residues, of which four putative zinc ligands (Cys and His) and several hydrophobic residues are strongly conserved. The yeast protein ADR1, a positive transcription regulator, contains two adjacent finger domains that have been implicated by deletion and genetic analysis as essential to the protein's function. Spectroscopic studies (UV/VIS, CD, 1D- and 2DNMR) on a synthetic ADR1 zinc finger domain indicate that the 30-residue peptide behaves as an independent folding domain in the presence of Zn^{2+}. Properties of the zinc finger domain and its solution structure will be presented.

T-AM-SymII-5 CONFORMATION, FOLDING AND HYDRATION IN PEPTIDES: RECENT INSIGHTS FROM CRYSTAL STRUCTURE ANALYSES.
Isabella L. Karle, Laboratory for the Structure of Matter, Naval Research Laboratory, Washington, D. C. 20375-5000.

The conformations of small linear peptides are readily affected by polarity of solvent, presence of water molecules, hydrogen bonding with neigboring molecules and other packing forces. Larger peptides have many intramolecular hydrogen bonds that outweigh the effects of intermolecular attractions. Polymorphs of apolar peptides (10-16 residues), grown from a variety of solvents, show a nearly constant helical conformation for each peptide consisting of 3-4 turns. The high resolution analyses of the crystal structures, 0.9 Å, provide conformational details. Transitions between a predominantly 3_{10}-helix and a totally α-helix occur for the same decapeptide in different polymorphs. For a decapeptide of a different sequence, with two independent molecules in a triclinic crystal, one of the molecules is entirely α-helical whereas the other not only has 3_{10}-type hydrogen bonds at either end, but the helix has become unwound at the N terminus. Head-to-tail hydrogen bonding of the helices occurs in a variety of motifs, ranging from three direct NH•••O=C bonds to only hydrogen bonds that are mediated by water or other solvent molecules. Hydration of completely apolar helices occurs by several different mechanisms. By one means, the helix is curved by the presence of a Pro residue by ~30-35°. At the bend, carbonyl oxygens extend away from the helix and attract water molecules that create a minipolar area on an otherwise hydrophobic surface. In another example, a water molecule is inserted directly into the helical backbone forming hydrogen bonds with an NH and O=C. The distortion of the helix exposes several other carbonyl oxygens to the exterior and attracts more water molecules. As a result, the apolar peptide mimics an amphiphilic helix and polar channels are formed in the crystal.

Tu-AM-A1 AUTONOMIC REGULATION OF A TIME-INDEPENDENT BACKGROUND CURRENT IN ISOLATED GUINEA-PIG MYOCYTES. Robert D. Harvey and Joseph R. Hume. Department of Physiology, University of Nevada School of Medicine, Reno, Nevada 89557.

Single myocytes isolated from guinea-pig ventricles were voltage-clamped using the whole cell patch-clamp technique. Exposure to isoproterenol (ISO) resulted in the generation of an apparently instantaneous background current (I_b) in more than 50 % of these cells. With calcium current blocked by nisoldipine and sodium current inactivated by a depolarized holding potential, I_b was most clearly observed as an instantaneous outward current elicited upon depolarization of the membrane to potentials greater than -20 mV, where, due to rectification, the normal background current (I_{K1}) is minimal. However, the difference current-voltage relationship was linear between -90 and +50 mV with a reversal potential near -40 mV. I_b disappeared upon concurrent exposure to acetylcholine (ACh) or washout of ISO, and the responses to ISO and ACh were blocked by propranolol and atropine, respectively. Forskolin also elicited I_b, suggesting that activation of adenylate cyclase is involved in the beta-adrenergic response. I_b was not affected by ouabain or glyburide, indicating that this current was not due to stimulation of the electrogenic Na,K-ATPase pump or activation of ATP-sensitive K^+ channels. In cells which exhibited I_b, no change in resting potential was observed, yet action potential duration was significantly shortened. The identity of this current is not known, but possible explanations include ISO activation of a previously unidentified channel or alteration of the properties of a known channel (e.g. I_{K1}). Supported by NIH grant HL 30143.

Tu-AM-A2 N. Buttner, A. Volterra and S.A. Siegelbaum. CONTROL OF S-K^+ CHANNEL ACTIVITY BY ARACHIDONIC ACID METABOLITES IN CELL-FREE INSIDE OUT PATCHES FROM APLYSIA SENSORY NEURONS. Center for Neurobiology and Behavior, Department of Pharmacology, Columbia University. Howard Hughes Medical Institute, 722 West 168th Street, New York, NY 10032.

Serotonin closes the S-K^+ channel of Aplysia sensory neurons through cAMP-dependent protein phosphorylation, whereas FMRFamide increases the open probability of the S channels through 12-lipoxygenase metabolites of arachidonic acid (a.a.) (Piomelli et al., Nature, 1987) and decreases the level of protein phosphorylation in sensory neurons (Volterra et al., Soc. Neurosci. Abstr., 1988). Here we test the ability of a.a. metabolites to modulate S channel activity in cell-free inside-out membrane patches.

Application of a.a. (20-50 μM) has little or no effect on S channel activity in the inside-out patches, suggesting that the cell-free patches cannot metabolize a.a. to an active metabolite. On average, the mean S current $\langle I \rangle$ in the patch after a 10-15 min exposure to a.a. is 0.9 ± 0.16 (n = 4) times the level of $\langle I \rangle$ before a.a. In contrast, 12-HPETE (20 μM), the unstable initial 12-lipoxygenase metabolite produces a reversible 3.14 ± 1.42 (n = 5) fold increase in mean S current within 4-7 min of its application. 12-HETE (20 μM), the stable breakdown product of 12-HPETE, has an intermediate action, causing a reversible increase in $\langle I \rangle$ to 1.65 ± .50 (n = 6) of control (4-7 min application). As the solution bathing the internal surface of the patch contains no ATP (or GTP), the reversible action of 12-HPETE cannot be explained by a phosphorylation or dephosphorylation reaction but may reflect a direct effect of a 12-lipoxygenase metabolite on the channel (see also Belardetti et al., Soc. Neurosci. Abstr., 1988).

Tu-AM-A3 Na^+ CURRENT-ACTIVATED K^+ CHANNELS REGULATE THE DURATION OF THE ACTION POTENTIAL IN RAT VENTRICULAR MYOCYTES. I.D. Dukes & M. Morad. Dept. of Physiol., U. of Penna. Sch. of Medicine, Philadelphia, PA.

In cardiac tissues of many species, including human, a transient outward current (i_{to}) can be recorded. In isolated rat ventricular myocytes, depolarizing clamp pulses from a holding potential of -80mV activated increasing amounts of this current, which was blocked by internal dialysis with Cs^+ or addition of 2mM 4-aminopyridine to the external solution, indicating its' homology with i_{to} recorded in other species. Analysis of the kinetics of activation suggested the existence of two components of i_{to}. The slowly activating component could be blocked by removal of Ca^{2+} from the external solution, or the addition of Ca^{2+}-channel blockers. Addition of TTX, greatly attenuated the rapidly activating component of i_{to}, as did substitution of external Na^+ with TRIS or choline. Inactivation of i_{Na} by conditioning depolarizing pulses also greatly suppressed this component of i_{to}. Replacement of Na^+ by Li^+, did not alter i_{to}, suggesting that activation of Na^+ channel rather than the presence of Na^+ was the important factor in the regulation of the rapidly activating component of i_{to}. Under current clamp conditions in the same myocytes, increasing the stimulation frequency caused a prolongation of action potential duration (APD). This effect was absent in the presence of 2 mM 4-AP, indicating it was secondary to suppression of i_{to}. Addition of TTX also caused a prolongation of APD which again could be prevented by 4-AP, suggesting a possible feedback mechanism between i_{Na}, i_{to} and APD. Such a mechanism may prevent excessive heart rates in the rat and could provide an alternative theoretical basis for the clinical efficacy of local anaesthetics as antiarrhythmic agents, if this current were to exist in the human. Supported by NIH #RO1 HL16152.

Tu-AM-A4 PINACIDIL-ENHANCED POTASSIUM CURRENTS IN VASCULAR SMOOTH MUSCLE ARE BLOCKED BY CHARYBDOTOXIN. H. Akbarali, D.A. Self, and K. Hermsmeyer, Chiles Research Institute, Providence Medical Center, and Oregon Health Sciences University, Portland, Oregon.

The vasodilatory effects of pinacidil on vascular smooth muscle may be mediated by opening of potassium channels. The effects of this drug on primary cultures of neonatal rat azygous vein smooth muscle cells were evaluated by recording whole-cell currents, using an Axopatch 1B amplifier. The external bathing medium consisted of (in mM): NaCl 130; $NaHCO_3$ 16; NaH_2PO_4 0.5; KCl 4.7; $CaCl_2$ 1.8; $MgCl_2$ 0.4; $MgSO_4$ 0.4; HEPES 13 and dextrose 5.5. The patch electrodes contained (in mM): KCl 145; $MgCl_2$ 0.5; HEPES 10 and EGTA 1. After an initial transient inward current, an outward potassium current was apparent on step depolarizations above -30 mV through +40 mV (holding potential of -90 mV). These currents did not time-inactivate during the test pulses (90 msec). The magnitude of whole-cell potassium currents exhibited a large (3-100X) increase on exposure to a 20 ul pulse of 10 uM pinacidil at all step depolarizations. The current-voltage curve was shifted upward and to the left by pinacidil. Further, resting membrane potentials hyperpolarized by at least 10 mV during the period of current enhancement by pinacidil. Both the baseline and pinacidil-enhanced potassium currents were unaffected by the presence of 100 mM TEA, but were 50% blocked by 5 ul of crude charybdotoxin. These observations suggest that pinacidil activates charybdotoxin-sensitive potassium channels in vascular smooth muscle.

Tu-AM-A5 THE MEMBRANE OF RAT PINEAL CELLS IN CULTURE CONTAINS AT LEAST TWO TYPES OF POTASSIUM CHANNELS. R. Etcheberrigaray, D.C. Klein and E. Rojas (Intr. by Charles Edwards) LMCN, NINCDS; LDN, NICHD; LCBG, NIDDK; National Institutes of Health, Bethesda, MD.

Potassium currents across the membrane of rat pineal cells in culture were measured using the patch clamp technique. Whole cell membrane currents (pipet solution (mM): 70 KCl, 70 Kaspartate, 10 K-Pipes, 5 Mg-ATP, 0.1 Na-EGTA at pH 7) exhibited both inward and outward currents. The analysis of the outward currents showed the presence of two kinetically different components, namely, an early transient and a delayed sustained current. In addition, the two components showed different steady-state characteristics and voltage sensitivity. The mid-point for activation of the early component (maximum chord conductance of 10.6 mS/cm^2) was -5 mV, and that of the delayed component (maximum chord conductance 8.8 mS/cm^2) was 20 mV. At the mid-point potential, while a 29 mV change in membrane potential induced an e-fold change in the magnitude of the transient component, a 41 mV change induced an e-fold change in the amplitude of the delayed component. The records of the single K-channel currents measured in the cell-attached mode (pipet solution (mM): 140 KCl, 1 $MgCl_2$, 2.6 $CaCl_2$, Na-hepes at pH 7.4) also revealed the presence of two types of K-channels in the patches (K-1 and K-2). The single channel conductances and fractional open times at resting potential different (110 pS and 0.12 respectively for K-1; 148 pS and 0.95 for K-2). The K-1 channels alone were activated by exposure of the inside of the membrane to Ca^{+2}; therefore we propose that the transient component of the whole cell membrane current is due to activation of the K-1 channels.

Tu-AM-A6 TRANSIENT POTASSIUM CHANNELS IN CHICK DORSAL ROOT GANGLION (DRG) CELLS J.L. Kenyon, S.K. Florio, M.R. Vasko, and R.J. Bauer. Dept of Pharm., U.T. Southwestern Med. School, Dallas, TX and Dept. of Physiol. Univ. of Nevada School of Medicine, Reno, NV 89557.

We used the patch-clamp technique to study voltage-activated transient potassium channels in primary cultured chick DRG cells. Cells were bathed in either NaCl superfusate or potassium aspartate superfusate while channel activity was recorded with pipettes filled with either NaCl or KCl solution. We found a class of channels that were not active at the resting potential but were activated transiently by depolarizations to potentials positive to -30 mV. The figure shows a typical recording made with NaCl in the bath and pipette. The membrane potential was depolarized 80 mV from the resting potential (estimated at -60 mV) for 200 ms at intervals of 3 s. The lower traces show 1.5 pA unitary currents and the upper trace shows the average of 100 such sweeps. In this experiment, the single channel conductance was 18 pS and the probability of channel opening peaked at 0.28 and declined to near zero with a time constant of 31 ms. With K in the bath and pipette, the time and voltage dependence of channel activity was unchanged, the single channel currents reversed near 0 mV, and the slope conductance was 40 pS. Thus, the channels are selective for K and are activated transiently by depolarization. In whole cell recordings, however, we were unable to detect transient outward current. This suggests that the patch-clamp does not always provide an accurate sample of membrane conductances. NIH HL26528 and AHA 87-648.

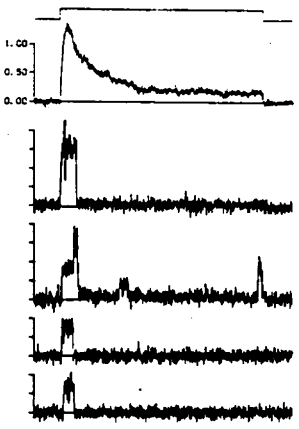

Tu-AM-A7 ION CHANNEL KINETICS: HAS IT BEEN PROVEN THAT CHANNELS HAVE ONLY A SMALL NUMBER OF STATES?

Larry S. Liebovitch, Dept. of Ophthalmology, Columbia Univ., College of Phys. & Surgeons, NY 10032

We proposed that single channel data are consistent with channels having a very large number (a continuum) of states. We found that the kinetic rate constants connecting these states have a fractal scaling. Korn and Horn; and McManus, Weiss, Spivak, Blatz, and Magleby recently reported that models with a few Markov states fit single channel data better than the simplest fractal model. Thus, they concluded that ion channels have only a few discrete states connected by independent, exponential time processes. However, our review of their analysis suggests that their conclusion is not supported by the arguments they present. First, extensive experimental and theoretical evidence over the last decade shows that proteins have a large number of states and can exhibit both exponential and non-exponential processes. Hence, it is no longer justified to assume, as they did, that there is always a small number of exponential rates. Second, their models fit the data not necessarily because they correspond to reality, but simply because they have a very large number of adjustable parameters (up to 15). We also show how the simplest fractal model can be generalized to better fit the data.

Supported by NIH EY6234, the Whitaker Foundation, and the American Heart Association.

Tu-AM-A8 A FAMILY OF PUTATIVE POTASSIUM CHANNEL GENES REVEALED BY A DELETION OF THE DROSOPHILA SHAKER GENE. Keith Baker, Aguan Wei, Alice Butler, Michael Pak, and Lawrence Salkoff (Intr. by Laurence Trussell), Department of Anatomy and Neurobiology, Washington University School of Medicine, 660 South Euclid Avenue, St. Louis, Mo 63110.

Voltage clamp recordings of Drosophila central neurons in mutant flies carrying a deletion of the gene coding for the Shaker potassium channel show that the majority of neurons in these mutant animals still have potassium currents similar to those coded by the Shaker gene. The Shaker-like currents present in these Shaker deletion mutants vary widely with respect to their kinetic properties. This suggests the presence of a family of Shaker-like genes in Drosophila. Using a Shaker cDNA probe and the technique of low stringency hybridization, three additional family members have now been isolated. The Shaker family genes are widely scattered in the genome. The deduced proteins of Shab, Shal, and Shaw have high homology to the Shaker protein; the sequence identity of the integral membrane portions is greater than 50%. The presumed gating charge regions for Shab and Shaw, however, are unusual in having some polar residues substituting for positively charged residues. It has now been found that Shaw, in addition to Shaker, has a close vertebrate homolog; thus, the individual members of the Shaker gene family probably evolved prior to the separation of vertebrates and invertebrates.

Supported by NIH grant RO1 NS24785-01 and a grant from the Muscular Dystrophy Association of America.

Tu-AM-A9 CHARYBDOTOXIN BLOCKS K^+ CHANNELS IN XENOPUS OOCYTES INDUCED BY FOUR DIFFERENT SHAKER cDNA CLONES. Rod MacKinnon, Christopher Miller, and Les Timpe, Graduate Dept. of Biochemistry, Brandeis University, Waltham, MA., and Howard Hughes Medical Inst., Dept. of Physiology, U.C.S.F., San Francisco, CA.

Charybdotoxin (CTX), a small protein purified from scorpion venom, is unique in its ability to block with nanomolar affinity several different types of K^+ channels. Previous work on the high-conductance Ca^{2+}-activated K^+ channel has provided a clear picture of the mechanism of block; CTX blocks this channel by physically occluding the externally facing entryway to the K^+ conduction pore. In addition, it is known that CTX interacts with several carboxyl groups in the channel mouth. Recently, it was shown that CTX also blocks a K^+ channel in Xenopus oocytes injected with transcript produced from a Shaker cDNA clone. The similarity of block in Shaker and Ca^{2+}-activated K^+ channels argues that CTX blocks these channels by a common mechanism. We are therefore in a position to examine the Shaker K^+ channel's external mouth with CTX. As a first step, we studied CTX block of four distinct Shaker channels. Oocytes were injected with transcript from Shaker A, B, C, and D, and the effect of CTX on the resulting K^+ currents was assessed. CTX blocks all four channels. For Shaker A, B, and D, the blocking affinities were quantitatively identical, with an inhibition constant of 3 nM for each. For technical reasons, it was impossible to determine quantitatively the CTX affinity for Shaker C, but block was qualitatively similar to that of the others. We are currently mutating putative external loop regions of Shaker in order to identify residues interacting with CTX, and hence lining the outer mouth of the channel.

Tu-AM-A10 SELECTIVITY AND PERMEANT ION EFFECTS ON GATING OF THE TYPE '*L*' K CHANNEL IN LYMPHOCYTES. by M.S. Shapiro & T.E. DeCoursey, Department of Physiology, Rush Medical Center, Chicago, IL 60612.

The voltage–gated type '*l*' K^+ channel superficially resembles delayed rectifier channels but profoundly differs in gating and kinetics. It was characterized in murine T lymphocytes (*J.Gen.Physiol.* 89:379, 1987), and has been seen in murine thymocytes, rat pulmonary epithelial cells, and the *Louckes* human lymphoma cell line. We here report the ionic selectivity of the channel and effects of permeant ion species on its gating. In whole–cell studies of murine MRL/*lpr* T–lymphocytes with 160 K^+ in the pipette and 160 *mM* bathing ion, the relative permeability sequence calculated from V_{rev} is K^+ (1.0) > Rb^+ (0.8) > NH_4 (0.14) ≥ Cs^+ (0.11) >> Na^+ (<0.005). Deactivation time constants with each of these ions carrying the current were (*ms* at $-100mV$ and 24°C) K^+ (.6) < NH_4^+ (1.5) < Rb^+ (4) < Cs^+ (8). The instantaneous inward conductance for Rb^+ was nearly half that for K^+. The inward NH_4^+ current was over ten times that for Cs^+ even though P_{rel} is nearly identical, as though Cs^+ can enter the channel as well as NH_4^+ but has a much longer occupancy time. Plotting peak conductance–voltage curves, activation is dramatically shifted to the left in Rb^+ ($V_{1/2} = -27mV$) compared to K^+ ($-9mV$) or NH_4^+ ($\approx 5mV$). Taken together, these results indicate that the type '*l*' channel is a multi–ion pore and that permeation and gating are not distinct, i.e., permeant ion species affects gating. In addition, it seems that some ions such as Cs^+ can get "stuck" in the channel as evinced by a very low conductance with Cs^+ as the charge carrier. *Supported by NIH grants SK04–HL01928 & R01–HL37500 (TD).*

Tu-AM-A11 Excess open–channel noise in the SR K^+ channel: effects of temperature and Mg^{2+}.
A.H. Hainsworth, R.A. Levis and R.S. Eisenberg.
Department of Physiology, Rush Medical Center, Chicago. IL 60612.

The large K^+ channel of the sarcoplasmic reticulum (SR) was studied in excised patches from single, split fibers of lobster remotor muscle. In the ± 100 mV range, single channel conductance is ≃ 200 pS at 20 °C. (In bath and pipette: 460 mM Kglutamate, 1.2 $CaCl_2$, 5.0 K_2EGTA, 1.0 MgATP, 0.9 $MgCl_2$, 25 HEPES: pH 7, 100 nM free Ca^{2+}, 1 mM free Mg^{2+}.) The open–channel noise has roughly constant power spectral density (S_0) up to 10 kHz. S_0 is close to the Johnson noise level when mean current (<i>) is relatively low (<i> ≃ 4 pA, V(applied) = 20 mV). As <i> increases, S_0 increases gently (slope < 1). When V(applied) = 50 mV, S_0 ≃ 3 times the ideal shot noise level, given by $2 \cdot q \cdot$<i> (q = unitary charge). With V(applied) = 50 mV, S_0 increases with temperature with a Q_{10} of 1.3. <i> also increases with Q_{10} = 1.3.

These results are consistent with open–channel noise produced by a combination of i) shot noise and ii) bandwidth–limited interruptions of the current (mean lifetime < 100 μs); both having a weak temperature dependence. Fast block by an aqueous ion could cause such interruptions. To reduce the free Mg^{2+} to trace activity, we omitted $MgCl_2$ and MgATP from the above recipe. There was no significant effect on <i> or S_0. Clearly, block by Mg^{2+} cannot explain the observed excess open–channel noise.

With V(applied) = 50 mV; 20 °C.	1 mM free Mg.	Trace free Mg.
<i>/pA:	9.0 – 9.5	9.1 – 9.7 (range)
$S_0/10^{-30}A^2/Hz$:	9.3 ± 1.4	9.4 ± 2.4. (S.D.)

Tu-AM-B1 X-RAY EVIDENCE FOR FOUR DIFFERENT CONFORMATIONS OF THE THIN FILAMENT

David Popp, Yuichiro Maéda & Kenneth C.Holmes
Max Planck Institute for med. research, Jahnstrasse 29, 6900 Heidelberg and
EMBL c/o DESY,Notkestrasse 85, 2000 Hamburg 52, FRG.

Taking the intensity change of the 2nd layer-line (LL) at a 1/19.2 nm axial and a 1/4.3 nm radial spacing as indicator for the thin filament structure we find 4 different conformations: 1) The relaxed or low Ca^{++} state, the intensity of the 2nd LL is about 7 % of the 5.9 nm LL intensity as revealed from rabbit psoas muscles in the relaxed state and from orientated gels of reconstituted rabbit thin filaments at Ca^{++} concentrations lower than pCa 6.9. 2) The high Ca^{++}state, the 2nd LL reaches 14 % of the 5.9 nm LL intensity in orientated gels of reconstituted thin filaments at Ca^{++} concentrations higher than pCa 6.75. Note that the transition occurs within 0.2 pCa units. In overstretched rabbit psoas muscles the transition occurs at the midpoint of the maximal force (around pCa 5.5). 3) The rigor state, rigor bridges induce a further increase of the 2nd LL in rabbit psoas up to 20 % of the 5.9 nm LL intensity. Addition of exogenious S1 to saturate all actin binding sites does not cause an additional change of the 2nd LL intensity. 4) The active state, in activated frog muscle the 2nd LL reaches about 40 % of the 5.9 nm LL intensity, 40 % of the change is induced by cycling crossbridges. Patterns from orientated gels of actin plus tropomyosin alone mimic this state. The radius of gyration (Rg) of cross-section of reconstituted thin filaments was measured to be 2.9 ± 0.1 nm independent of the Ca^{++} concentration indicating that there is if any, only a small radial movement of tropomyosin on activation.By comparing the Rg of F-actin with the Rg of F-actin plus tropomyosin, it is deduced that the tropomyosin strands are centred at 3.5 nm from the filament axis.

Measurements on activated muscle and solution scattering experiments were performed at the EMBL X33 beam-line, static measurements on muscles and orientated gels were done on a rotating anode using a Xentronix 2-D detector.

Tu-AM-B2 STRUCTURAL STUDIES OF THE TROPOMYOSIN/TROPONIN SWITCH BY CRYOELECTRON MICROSCOPY AND X-RAY DIFFRACTION.

D. Cabral-Lilly*, G.N. Phillips, Jr.[+], G. Sosinsky*, L.A. Melanson* and C. Cohen*. *Rosenstiel Basic Medical Sciences Research Center, Brandeis University, Waltham, MA 02254. [+]Department of Biochemistry, Rice University, Houston, TX 77251.

Cryoelectron microscopy coordinated with X-ray diffraction is being used to visualize the structure of troponin and its interactions with tropomyosin. The low resolution crystallographic structure of the tropomyosin/troponin complex has been determined (White, S.P., Cohen, C. and Phillips, G.N., Jr., Nature 325:826, 1987), but molecular motions in the co-crystal lattice diminish the visibility of the head region of troponin. Tropomyosin crystals embedded in vitreous ice show remarkable contrast and order with computed transforms extending to about 18 Å resolution. Micrographs of the two-dimensional projection of the [100] view have been digitized, transformed and corrected for lattice distortions by correlation analysis. In a preliminary comparison with X-ray diffraction data from the same crystals (Phillips, G.N., Jr., Fillers, J.P. and Cohen, C., J. Mol. Biol. 192:111, 1986), the X-ray amplitudes were attenuated by applying a large temperature factor to simulate the effects of the electron microscope contrast transfer function at low resolution. The resulting electron microscope and X-ray data show good correspondence. These results provide the basis for analysis of the structure of troponin incorporated into the crystal lattice. Troponin is clearly visible in recent images of co-crystals, and its conformational changes with calcium may be detectable.

Tu-AM-B3 THE EFFECT OF TERTIARY STRUCTURE ON THE OPTICAL ROTATORY PROPERTIES OF TROPOMYOSIN: A THEORETICAL STUDY

Thomas M. Cooper, Dept. of Biochemistry, Colorado State University, Ft.Collins CO, 80523, USA

Tropomyosin, in the coiled coil state, has a negative circular dichroism(CD) band at 280 nm, associated with the phenolic L_b transition. The protein contains 6 tyrosines per α-helical chain, with poorly understood contributions to the CD spectrum. The optical rotatory properties of the tyrosine L_b transition were modeled as two 21 residue α-helices distorted to a coiled coil conformation with one tyrosine per chain. Rotational strength was calculated using strong coupling exciton theory with two transitions($n\pi^*,\pi\pi^*$) per amide chromophore and four transitions(L_b,L_a,B_b,B_a) per tyrosine. For heptet positions a to g, the L_b transition rotational strength surface was calculated for all possible side chain dihedral angles. The following predictions are made from the results. Tyrosines in heptet positions b,c,e,f and g will have optical properties similar to those of a tyrosine attached to a single helix. From simple assumptions about tyrosine conformation, the L_b transition rotational strength will be negative for positions b,c,e,f and g. The optical properties of tyrosines in positions a and d will reflect the degree of coupling between the phenolic rings and the helices. In a rigid coiled coil, positions a and d will be spectroscopically distinguishable. Optical rotation of N-terminal tyrosines(Y60, perhaps Y162), will behave according to a rigid coiled coil model. Because of conformational fluctuations and solvation of the phenolic rings, the optical rotation of C-terminal tyrosines(Y214,Y221,Y261,Y267) will behave like a tyrosine attached to a single helix and have a negative rotational strength. (This work was supported by USPHS grant GM 22994 and a grant of computer time from the CSU Computer Center.)

Tu-AM-B4 THE STATE OF RECONSTITUTED THIN FILAMENTS IS MONITORED BY THE EXCIMER FLUORESCENCE OF PYRENE-IODOACETAMIDE LABELED TM. Y. Ishii & S.S.Lehrer, Boston Biomedical Research Institute, Boston MA.02114.

The change in state of tropomyosin (Tm) on the muscle thin filament induced by the binding of myosin subfragment-1 (S1) involves a change in environment of the Cys 190 region of Tm (Ishii & Lehrer, Biochemistry 24, 6631,1985; 26, 4922, 1987), and a change in geometry between Tm and actin (Lehrer & Ishii, Biochemistry 27, 5899,1988). We now report measurements of the excimer (E) fluorescence of pyrene-iodoacetamide labeled Tm (PIA-Tm). The E fluorescence of PIA-Tm bound to F-actin was enhanced 2X by the binding of S1 to actin and was half complete at ~1 S1/ 7 actins. The binding of S1-MgADP or S1-MgAMPPNP to actin-PIA-Tm produced the same E fluorescence change as in the absence of nucleotide even though the binding was weakened. The E fluorescence of the reconstituted thin filament (actin-PIA-Tm-troponin) depended upon the salt concentration in the absence and presence of S1. The E fluorescence vs [S1] profile of the reconstituted thin filament at 0.25 M NaCl was Ca^{2+}-dependent, i.e., more S1 binding was required to shift the Tm state in the absence of Ca^{2+} in agreement with the cooperative binding model (Hill et. al., PNAS 77, 3186, 1980). These probe studies indicate that: i.) the E fluorescence of PIA-Tm monitors the Tm-state change induced by S1 binding, ii.) the strong binding state of Tm induced by S1 is nucleotide-independent. (Supported by NIH and NSF).

Tu-AM-B5 UNFOLDING AND REFOLDING STUDIES OF FROG TROPOMYOSINS. S.S. Lehrer*, Y.Qian* & S. Hvidt#
*Boston Biomedical Research Institute, Boston MA; #Riso National Laboratory, Roskilde, Denmark

Frog tropomyosin isolated from *R. esculenta* leg muscle, consists of α & β chains. The α-chains have the greater mobility on SDS-PAGE. The thermal unfolding profiles of the three coiled-coil dimers, αα, αβ & ββ at 0.5 mg/ml in 0.5 M NaCl, 1 mM EDTA, 1mM dithiothreitol, 20 mM Na phosphate buffer, pH 7.0, were studied by circular dichroism (CD) at 222 nm. αβ and αα were isolated in the native form by hydroxyapatite chromatography, and ββ was renatured from separated chains by urea-ion exchange chromatography at pH 4.0. At 5°, αα and αβ were >95% helical but ββ was only about 70% helical. Whereas αα & ββ unfold in single transitions at 49° and 32°, respectively, αβ unfolds in two ≈ equal transitions at 37° and 49°. (*R. temporaria* αβ also unfolds in two transitions, Hvidt, Biophy. Chem. 24, 211, 1986). *Esc.* αα & ββ molecules refolded reversibly from separated chains at high temperature or GdmCl. Attempts to refold *esc.* αβ molecules from GdmCl or high temperatures produced an ≈ equal mixture of refolded homodimers, αα & ββ. These studies provide evidence for chain exchange and dissociation and that *in vitro* renaturation of *esc.* αβ, the principal *in vivo* species, is not readily accomplished. (Supported in part by NIH).

Tu-AM-B6 EVIDENCE FOR PERIODIC ACTIN BINDING SITES ON TROPOMYOSIN. S. E. Hitchcock-DeGregori and T. Varnell, UMDNJ-Robert Wood Johnson Medical School, Piscataway, NJ 08854.

In muscle, tropomyosin (TM), an α-helical coiled-coil protein, spans the length of seven actin monomers in the thin filament. Sequence analysis (by others) of outer helical residues in the coiled coil has revealed periodicities sufficiently regular to correspond to seven, or possibly two sets of seven (14), quasi-equivalent actin binding sites. In order to test the hypothesis of periodic actin binding sites experimentally, we used oligonucleotide-directed mutagenesis to make deletions in chicken striated α-TM that correspond to 0.5, 0.67 and one actin binding site, based on there being seven sites. The deletions are of the second site, encoded mostly by the second exon: Res. 47-67, 47-74, 47-88. The lengths of the deletions are multiples of seven amino acids in order to retain the coiled-coil structure of the proteins. Consequently, the largest deletion is 42 instead of 39.3 residues for precise removal of the site. Recombinant TMs were expressed in E. coli as fusion proteins, the form that binds well to actin (Heald and Hitchcock-DeGregori, 1988, J. Biol. Chem. 263, 5254-5259). The proteins were labeled with ^{14}C-NEM for determination of binding constants by cosedimentation. The affinity of wildtype tropomyosin (K_{app}=4.2±1.5x10^6M^{-1}) was about four-fold higher than the TM with one site removed (1.1±0.5x10^6M^{-1}). The affinity of the two shortest deletions was <<10^5M^{-1}, too weak to measure accurately using our assay. The results prove the existence of two or more specific actin binding sites, one on each site of the deletion, and are consistent with the existence of seven quasi-equivalent sites. In the presence of troponin, the affinities of wildtype and d47-88 TMs are the same (7.4±3.0x10^6M^{-1}), much higher than that of the two other deletions (3.0±4.5x10^5M^{-1}). Supported by NIH-HL35726 and the American Heart Association.

Tu-AM-B7 EFFECT OF PHOSPHORYLATION ON THE INTERACTION AND FUNCTIONAL PROPERTIES OF RABBIT STRIATED MUSCLE αα TROPOMYOSIN. David H. Heeley*, Mark H. Watson**, Alan S. Mak**, Pierre Dubord* and Lawrence B. Smillie*. *Department of Biochemistry, University of Alberta, Edmonton, Alberta, T6G 2H7 Canada and **Department of Biochemistry, Queen's University, Kingston, Ontario K7L 3N6 Canada.

Samples of rabbit cardiac αα tropomyosin containing 0.95 mole of phosphate per mole of monomer have been prepared enzymatically (Montgomery, K. and Mak, A.S. (1984) J. Biol. Chem. 259, 5555-5560) or by fractionation of the phosphorylated and nonphosphorylated forms on a FPLC Mono Q column in 9 M urea, 50 mM Tris, pH 8.0. Although phosphorylation did not alter the F-actin binding properties of tropomyosin, the phosphorylated protein had substantially higher viscosities at low ionic strengths indicating a greater propensity for head-to-tail interaction. When the effect of whole troponin on this interaction was investigated, a reduced level of polymerization was observed for the phosphorylated derivative even though phosphorylation somewhat increased the binding of whole troponin and troponin-T to tropomyosin, as demonstrated by affinity chromatography. In a reconstituted actin (4 μM) plus myosin subfragment 1 ATPase assay (50 mM ionic strength), significantly higher activities over a range (1 to 8 μM) of subfragment 1 concentrations were observed with phosphorylated tropomyosin compared with the nonphosphorylated protein, both alone, and also in the presence of troponin (plus Ca^{2+}). Crucially, when these measurements were repeated with a sample of phosphorylated tropomyosin which had been pretreated with alkaline phosphatase, the differences in rate were eliminated. This is the first demonstration of an effect of phosphorylation on the functional properties of tropomyosin. (Supported by the Medical Research Council of Canada.)

Tu-AM-C1 Complex Formation Between CrATP and the SR ATPase in the Absence of Ca^{2+}. Zhida Chen, Lee Fielding, Carol Coan, and Gail Cassafer, Dept. of Physiology, Univ. of the Pacific, 2155 Webster St., San Francisco, CA 94115.

Ligand exchange interactions between CrATP and transport ATPases are generally characterized by slow reaction kinetics and high stability. It has been demonstrated that CrATP will undergo ligand exchange with the SR ATPase under conditions where a phosphorylated enzyme intermediate is normally formed (Serpersu, E. H., Kirch, U., & Schoner, W., 1982, Eur. J. Biochem. 122, 347-354). We find that a similar complex can be formed in the absence of Ca^{2+}, although the rate of ligand exchange under these conditions is much slower; k(Ca) = .1 min^{-1} vs k(EGTA) = .02 min^{-1}. Increased temperature (37 C vs 25 C) is used to drive the reaction. 4.0 + .5 nmol/mg (^{32}P)CrATP•E can be formed; a number equal to maximal levels of E-P which can be formed with MgATP in our preparations. Inhibition by Pi and VO_3 demonstrates a requirement for the phosphorylation site. SDS gel electrophoresis of tryptic fragments shows the (^{32}P) to be primarily on the A1 fragment.

Ca^{2+} binding to high affinity sites on the SR ATPase is a stringent requirement for phosphorylation by MgATP. Our ability to form a complex in the absence of Ca^{2+} with CrATP, which has many of the characteristics of a phosphoenzyme, appears to be due to the high stability of the ligand bond formed between Cr and the enzyme ($k_{off} < .002\ min^{-1}$).

Tu-AM-C2 **MAPPING OF AN ARGININE RESIDUE TO A DISCRETE REGION OF THE NUCLEOTIDE SITE OF SARCOPLASMIC RETICULUM Ca^{2+}-ATPase***

James E. Bishop, Univ. of Maryland Medical School, Dept. of Biological Chemistry, Baltimore, MD 21201.

Studies were undertaken to chemically modify and map arg residue(s) within the nucleotide site of SR Ca^{2+}-ATPase: to identify the discrete portions of the ATP molecule with which they interact. A novel approach was developed, exploiting the high affinity binding properties of the TNP-nucleotides. Analogous to TNP-ATP, TNP-ADP, and TNP-AMP which are all known to bind to the nucleotide site with K_d's < 0.1 μM, the adenosine analog, TNP-Ado, was likewise found to bind to the nucleotide site, but with a lower affinity, K_d = 3 μM.

The Ca^{2+}-ATPase was reacted with 5 mM phenylglyoxal, an arg-specific reagent, at pH 8 and 25°C for various times. This caused loss of the ability of TNP-ATP to bind, with a half-time of 6 min. Thus, localization of at least one arg residue to the nucleotide site was concluded.

This modification also caused the loss of the binding abilities of TNP-ADP and TNP-AMP with identical time courses to that of TNP-ATP. In contrast, the binding ability of TNP-Ado was completely retained. Therefore, only triphosphate region arg residue(s) were modified, certainly at the α-phosphate position and possibly, in addition, at the β- and/or γ-phosphate positions.

The stoichiometry of TNP-ATP protectable modification was measured to be 1.2 mol modified arg per mol Ca^{2+}-ATPase, using [^{14}C]phenylglyoxal. Thus, the possibility of more than one modified arg residue within the triphosphate-binding region of the site was excluded.

It was concluded that the nucleotide site contains a single arg residue, which is located at the α-phosphate position. Experiments are in progress to localize the modified arg to the primary structure of the Ca^{2+}-ATPase.

*Supported by the Frank C. Bressler Research Fund and University of Maryland Direct Research Initiative Fund.

Tu-AM-C3 THE EFFECTS OF TRYPSIN DIGESTION ON SARCOPLASMIC RETICULUM(SR) ACTIVE AND PASSIVE CA^{2+} TRANSPORT. Chengjing Cao, Tim Lockwich, Adil E. Shamoo; Dept. of Biol. Chem., School of Medicine, Univ. of Maryland, Baltimore, MD 21201.

Trypsin digestion of intact SR vesicles and reconstitution of the purified ATPase from the digested SR into sealed vesicles were carried out. The "uncoupling" of Ca^{2+} transport from ATP hydrolysis was studied through the determinations of Ca^{2+} uptake and Ca^{2+} efflux in SR vesicles or the reconstituted proteoliposomes, hydrolysis activity of Ca^{2+}-ATPase, and analysis of gel electrophoresis. The results show that the effect of trypsin digestion on SR Ca^{2+} uptake is related to cleavage levels of ATPase. The change of Ca^{2+} uptake in the reconstituted vesicles and analysis of gel electrophoresis for the purified ATPase from the digested SR are consistent with those events occuring in SR vesicles. However, a marked decrease in hydrolytic activity of ATPase cannot be detected even though Ca^{2+} uptake was decreased by more than 90% at TD2 cleavage. Also, no difference in the ATP dependence of hydrolytic activity was seen between SR and trypsin-treated SR. The passive Ca^{2+} efflux rate for tryptically digested SR is much larger than SR control in the presence of Mg+ruthenium red. No significant difference, however, was found between SR and tryptically digested SR in the absence of Mg+ruthenium red or in the presence of ATP. These results imply that tryptic digestion of SR opens the Ca^{2+} channel despite the presence of Ca^{2+} Channel inhibitors Mg+ruthenium red.

Tu-AM-C4 **A Fluorescence and DSC Study of the Influence of Sensitizers and Protectors on the Thermal Inactivation of the Ca^{+2}-ATPase of Sarcoplasmic Reticulum**

CHING ZHANG AND JAMES R. LEPOCK, DEPARTMENT OF PHYSICS, UNIVERSITY OF WATERLOO, WATERLOO, ONTARIO, CANADA, N2L 3G1.

The mechanism of thermal inactivation of the Ca^{+2}-ATPase of rabbit SR was investigated and related to the thermal denaturation of the enzyme. Ca^{+2} -transport and ATP hydrolysis was measured after exposure to 35 - 50 °C and compared to the thermal unfolding as measured by fluorescence spectroscopy and differential scanning calorimetry (DSC). Tryptophan (present in transmembrane domain) fluorescence and FITC (labels the ATP binding site) fluorescence were used to show that the enzyme denatures through two domains. The specific interaction of the agents glycerol, ethanol, deoxycholate (DOC), and 2,6,-di-tert.-butyl-4-methylphenol (BHT) with the protein-lipid membrane was determined by the effects on thermal inactivation of activity, denaturation, and lipid physical properties (fluidity). The latter property was determined from the rotational anisotropy of the fluorescent probe diphenylhexatriene (DPH) and the motional parameters of alkane and fatty acid spin labels. Glycerol protects and ethanol sensitize the enzyme to both denaturation and inactivation. Both agents appear to interact directly with the Ca^{+2}-ATPase since they have little effect on lipid orgnization. DOC solubilizes the membrane and at high concentration lower the denaturation midpoint temperature (T_m) of both domains of the Ca^{+2}-ATPase by 8°C. BHT a potent lipid perturber sensitizes to inactivation of Ca^{+2}-transport and lowers the T_m of the transmembrane domain, probably through alteration of the lipid-protein interaction. Vesicular structure and the T_m of the cytoplasmic domain is unaffected. Thus, each of these agents appears to interact with the Ca^{+2}-ATPase by a different mechanism.

Tu-AM-C5 **Ca^{2+}-ATPase ORGANIZATION IN PHOSPHORYLATED SCALLOP SARCOPLASMIC RETICULUM**, Peter Hardwicke* and John J. Bozzola†, *Dept. of Medical Biochemistry and †Center for Electron Microscopy, Southern Illinois University, Carbondale, Illinois 62901-4409.

Scallop FSR was phosphorylated with P_i to the ADP-insensitive (E_2P) form, and with ATP to a 92:8 mixture of E_1P:E_2P. Examination of the material by negative staining in the electron microscope showed a quasi-crystalline lattice with single strands of Ca^{2+}-ATPase molecules running in the surface of the membranes. The unit cell dimensions in FSR tubular vesicles flattened into the carbon film were a = 51 Å, b = 60 Å, $\gamma \sim 90°$. The size of the unit cell is only large enough to accomodate a single Ca-ATPase molecule (P1 lattice). This is in contrast to previous studies of the scallop FSR negatively stained under relaxing conditions (Castellani and Hardwicke, 1983; Castellani, Hardwicke and Vibert, 1985), where a P2 lattice was present in flattened tubes, with the enzyme arranged into ribbons of dimers. On dephosphorylation of the E_2P tubes by addition of K^+, followed by addition of substrate or substrate analogues in the effective absence of free Ca^{2+}, in the presence of Mg^{2+}, the E_2P P1 lattice was converted to a P2 lattice (dimer ribbons). Therefore, transition from the E_2P state of the FSR to the "relaxed" state may involve rotation of Ca-ATPase subunits in the membrane. The "dimeric" P2 lattice state of the scallop FSR may function as a way of stabilising the unphosphorylated Ca-ATPase molecules in the membrane, when the Ca^{2+} binding sites are empty. NSF Grant DCB-8509699

Castellani, L. and Hardwicke, P. M. D. (1983) J. Cell Biol., 97, 559-561.
Castellani, L., Hardwicke, P. M. D. and Vibert, P. (1985) J. Mol. Biol., 185, 579-594.

Tu-AM-C6 FITC DOES NOT PREVENT THE INHIBITION OF GTPASE ACTIVITY BY ATP IN CARDIAC SARCOPLASMIC RETICULUM. C.A. Tate, S. Blaylock, E. Hudson, A. Chu, R.B. Bick, and M.L. Entman. Dept. of Med., Baylor College of Medicine, Houston, TX 77030.

In cardiac sarcoplasmic reticulum (SR), we previously showed that in contrast to the hydrolysis of ATP, the hydrolysis of GTP is not sensitive to Ca^{2+} and does not involve a Ca^{2+}-dependent phosphoenzyme. GTP may be hydrolyzed by the CaATPase because (1) GTPase activity is inhibited by either ATP or AMP-P(NH)P in a noncompetitive fashion with Ki = 1-5 μM, and (2) GTP induces Ca^{2+} accumulation into a pH and ionophore-sensitive pool held in common with ATP-dependent Ca^{2+} accumulation. In the present study the CaATPase was labelled with fluorescein isothiocyanate (FITC) which inhibited the CaATPase activity (I_{50} = 16 μM at pH 7 and 25°C) with 100% inhibition at 60 μM FITC. Similarly, Ca^{2+}-sensitive phosphoenzyme and ATP-induced Ca^{2+} accumulation were not observed at 60 μM FITC. However, the MgATPase activity was minimally affected. Ca^{2+} accumulation with GTP was also completely prevented by 60 μM FITC even though FITC only inhibited GTPase by 10-20% regardless of the presence of Ca^{2+}. Surprisingly, ATP and AMP-P(NH)P still inhibited the GTPase activity in the presence of 60 μM FITC with a Ki = 1-2 μM. The data indicate that in cardiac SR, FITC does not label the ATP binding site *per se* but may prevent Ca^{2+}-induced conformational changes. (Supported by NIH, HL 13870 and AG 06221.)

Tu-AM-C7 GLOBAL ISCHEMIA AFFECTS THE CALCIUM RELEASE CHANNEL OF CARDIAC SARCOPLASMIC RETICULUM. W.R. LeBolt, N.H. Manson, and J.J. Feher. Department of Physiology, Medical College of Virginia, Virginia Commonwealth University, Richmond, VA 23298

The specific character of the ischemic damage to the cardiac SR has not yet been identified. We assayed SR function after various periods of global ischemia by the oxalate-supported calcium uptake rate of whole heart homogenates. This method avoids possible artifacts in the isolation of the SR. This assay was also performed in the presence of 20uM ruthenium red or 500uM ryanodine to specifically block the SR calcium release channel. Ischemia was produced in both an in situ preparation and in a Langendorff preparation. Global ischemia of 10min or more produced in either model caused a statistically significant depression of calcium uptake rate measured in the absence of Ca channel blockers. The similar effect of ischemia produced in the two models suggests that blood-borne elements are not responsible for ischemic damage. The depression in calcium uptake rate was not observed when ryanodine or ruthenium red was present in the assay medium. This result suggests that the Ca-ATPase and permeability barrier of the SR membrane is not affected significant ly by ischemia, but the Ca release channel is open after ischemia. This effect is long-lived, as it was not reversed by exposure to the normal preincubation and assay conditions. After 30min of global ischemia, 10min of reperfusion resulted in recovery of normal rhythm and contraction in 10 of 15 hearts. The calcium uptake rate also recovered in these 10 hearts. Thus, ischemic damage of the Ca release channel correlates well with gross ischemic dysfunction. Supported by NIH grant HL34681.

Tu-AM-C8 MASS MEASUREMENT OF THE FEET STRUCTURES/CALCIUM RELEASE CHANNEL OF SARCOPLASMIC RETICULUM BY SCANNING TRANSMISSION ELECTRON MICROSCOPY (STEM). Akitsugu Saito, Makoto Inui, Joseph S. Wall* and Sidney Fleischer. Dept. of Molecular Biology, Vanderbilt University, Nashville, TN 37235 and *Biology Dept., Brookhaven National Laboratory, Upton, NY 11973.

The calcium release channel (CRC)/ryanodine receptor which triggers calcium release in excitation-contraction coupling has been localized to the terminal cisternae (TC) of sarcoplasmic reticulum. The CRC has been isolated and identified structurally as the feet structures which are involved in junctional association of the TC with the transverse tubule to form the triad junction. Thus, the feet structures serve both as a junctional component involved in signal transmission and as CRC. The feet structures approximate square prisms of about 260 x 260 x 150 Å, and consist of an oligomer of a single high molecular weight polypeptide (HMP) with Mr estimated by SDS-PAGE to be from 360 to 450 KD. This study is concerned with measurement of the mass of the feet structures from fast twitch skeletal muscle using STEM. Images were obtained by dark field of the unstained freeze-dried samples using a large angle annular detector. No correction was made for detergent and salt in the sample since the mass and the shape of the internal control (TMV) appeared uneffected in the areas selected. Similar results were obtained with or without glutaraldehyde fixation. We find a mass of 2.3 ± 0.3 megadaltons. Considering the range of Mr of the HMP, the number of polypeptides/foot structure calculates to be 4.4 to 7.2. STEM measurements of the monomer should help resolve whether the structure which appears to have four-fold symmetry conforms to a tetramer or an octamer. [Supported in part by NIH DK 14632, and Muscular Dystrophy Association to SF and US DOE and NIH RR01777 to JSW.]

Tu-AM-C9 THE FOOT PROTEIN IS ANCIENT. Clara Franzini-Armstrong* and Loriana Castellani‡. * Dept of Anatomy, University of Pennsylvania, Philadelphia, Pa. 19104; ‡Rosenstiel Research Center, Brandeis University, Waltham, Mass. 02254.

The foot protein forming the junction between transverse tubules and sarcoplasmic reticulum (SR) in skeletal muscle fibers of vertebrates is an unusual calcium channel, with a very large cytoplasmic domain. The entire molecule has a four fold symmetry and the cytoplasmic domain has a tetrafoil or four leaf clover shape, i.e., it is composed of four subunits with a spherical outline surrounding a central depression. We have studied the structure of the foot protein by freeze-drying and rotary shadowing crude SR fractions isolated from the fast adductor of the scallop (Placopecten m.). In this muscle the SR forms frequent peripheral couplings with the surface membrane. the couplings are functionally equivalent to T-SR junctions and have junctional feet. In the isolated SR the crystalline calcium ATPase, which covers the entire surface of free SR, abruptly terminates at the edges of the junctional SR leaving a membrane domain occupied only by junctional feet. Feet have a tetrafoil structure and dimensions identical to those from vertebrate muscle. Mollusca diverge from Vertebrata very early in the phylogenic tree, therefore we conclude that the foot protein must have been present in primitive organisms. General conformation and function of the protein have been maintained. Supported by NIH HL 15835 to Pennsylvania Muscle Institute, AR17346 to C. Cohen and NSF DMB 85-02233 to C. Cohen and P. Vibert.

Tu-AM-C10 SUBUNIT STRUCTURE OF THE SKELETAL MUSCLE RYANODINE RECEPTOR-Ca^{2+} RELEASE CHANNEL COMPLEX. F. Anthony Lai, H. Amy Smith and Gerhard Meissner. Department of Biochemistry, University of North Carolina, Chapel Hill, NC 27599-7260.

The ryanodine receptor-Ca^{2+} release channel from rabbit skeletal muscle sarcoplasmic reticulum (SR) has been purified to apparent homogeneity in Chaps detergent as a large protein complex of ~30S. The complex possessed a single high-affinity binding site for [^{3}H]ryanodine (K_D=4 nM, 540 pmol/mg protein) and comprised one major protein band of M_r ~400,000 (Lai et al., Nature 331, 315, 1988). The purified 30S complex was radioiodinated and found to migrate as a single peak with an apparent sedimentation coefficient of ~30S and ~10S upon density gradient centrifugation and with pI of ~3.7 and ~4.0 upon 2D gel electrophoresis in Chaps and Zwittergent 3-14, respectively. [^{3}H]Ryanodine binding to SR membranes in 50 µM - 1 mM free Ca^{2+} and mM adenine nucleotide revealed the presence of both high-affinity (K_D=7 nM, n_H=1) and low-affinity (n_H ~0.4) sites with a ratio of 1:3. Trypsin digestion of membranes or reduction of free Ca^{2+} to <0.1 µM in the binding assay resulted in loss of high-affinity but not low-affinity ryanodine binding. In Hill plots, the data could be reasonably well fitted by a straight line with n_H=0.8 and K' ~10000 nM. These studies are compatible with a subunit structural model of the SR ryanodine receptor-Ca^{2+} release channel complex of four identical polypeptides of M_r ~400,000. Supported by MDA Fellowship (FAL) and NIH grant AR18687.

Tu-AM-C11 **Ca^{2+} CHANNELS FROM SARCOPLASMIC RETICULUM (SR) OF SPLIT LOBSTER MUSCLE FIBERS.** J. Wang, J. M. Tang and R. S. Eisenberg. Department of Physiology, Rush Medical College, Chicago, Il 60612.

Fibers of the second antenna remotor muscle of lobster were split in relaxing Ringer (high K^+, low Ca^{2+}) to expose the membrane surface of the SR for patch clamp recording. A perfusion pipette within the patch pipette is used to exchange the pipette (cytoplasmic) solution while the membrane remains sealed. Two types of Ca^{2+} channels were seen in 5–10% of excised patches. The conductance of large and small Ca^{2+} channels, measured in 53 mM Ba^{2+}, are ≃100pS and ≃15pS, respectively. The large channel occasionally enters sub-conductance states. The large Ca^{2+} channel looks "cleaner" in Ba^{2+} than in Ca^{2+} solution (see illustration). The selectivity for Ba^{2+} versus Ca^{2+} is ≃1.7 (conductance ratio). Ryanodine action is concentration dependent. 15 µM ryanodine (cytoplasmic side) locks the large Ca^{2+} channel into a long lasting sub-conductance state with some excursions to the closed and fully open state. Ryanodine has no obvious effect on the SR lumenal side of the channel. 10 mM caffeine had no dramatic effects on open channels, when applied to SR lumenal side or cytoplasmic side.

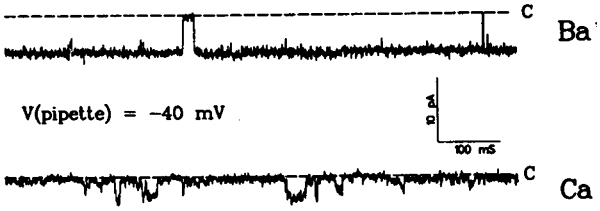

This lobster preparation can also be studied using "on SR" recording; its channels are then less likely to be separated from their regulators.

Tu-AM-C12 **VERAPAMIL, A T-TUBULE CALCIUM CHANNEL BLOCKER, INHIBITS RYANODINE BINDING AT THE TRIAD JUNCTION OF SKELETAL MUSCLE.** Hector H. Valdivia and Roberto Coronado. Department of Physiology and Molecular Biophysics, Baylor College of Medicine, Houston, Texas 77030.

T-tubules connected to the terminal cisternae of SR in skeletal muscle serve to propagate the nervous stimulus for muscle contraction. Triad junctions, a preparation where T-tubule membranes remain intimately associated with those of the SR, represent a valuable model to examine the possible interactions between tubular proteins and the feet structures of SR. We describe here an inhibitory effect of the T-tubule calcium channel blocker Verapamil on Ryanodine (RyD) binding, a ligand of the SR Ca-release channel. Purified triads (Mitchell, et al., J. Cell Biol. 96:1008) exhibit [3H]RyD and [3H]PN200-110 binding with a Kd of 7 nM and 0.9 nM and a Bmax of 9 and 12 pmol/mg protein, respectively. In competition experiments, Verapamil, but not Nitrendipine nor Diltiazem, displaced >90% of [3H]RyD binding with an IC_{50} of 4-10 µM. The displacement is enhanced at pH 8 to 9, a range that is optimal for [3H]Verapamil binding to its T-tubule receptor. When assayed at different [Ca^{2+}], [3H]RyD binding displays a bell-shaped curve with an optimal at 30-100 µM. However, the binding is drastically decreased and becomes Ca-independent when the preparation is incubated with 20 µM Verapamil (See figure). Upon solubilization of triads or in purified "heavy" SR, there is no effect of verapamil on [3H]RyD binding, suggesting that such modulation requires a component of the tubular membrane attached to the SR membrane. Supported by AHA, MDA and NIH.

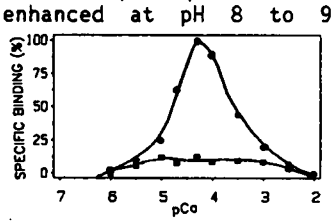

Tu-AM-D1 CARBOHYDRATES AT CELL SURFACES: MOTION AND DYNAMICS AS VISUALIZED BY ^2H NMR. Ian C.P. Smith, John Baenziger, Michèle Auger and Harold C. Jarrell. Division of Biological Sciences, National Research Council, Ottawa, Canada K1A 0R6

The carbohydrates on cell surfaces are involved in a multitude of interactions with other cells, antibodies, hormones and drugs. ^2H NMR of labelled carbohydrates can reveal accurate details about organization and dynamics, even in a precipitated system. We have prepared a series of specifically deuterated glycolipids, and analyzed their ^2H NMR spectra in lamellar dispersions and in hexagonal mesophases. The molecular order parameter, the molecular location of the axis of motional averaging, and the orientation of this axis with respect to the plane of the lipid bilayer have been determined. The order parameters and locations of the ordering axes vary significantly from one carbohydrate framework to another and are very sensitive to the nature of the glycosidic link. Conversely, in all systems studied the axis of motional averaging is found to be normal to the plane of the bilayer. The exocyclic moieties of the carbohydrate residues manifest more than one rotamer in slow exchange on the ^2H NMR time scale (10^4 s^{-1}). The ^2H NMR parameters respond to interaction of the cells with anesthetics and allow a very detailed molecular interpretation of lipid-anesthetic action.

At the level of the acyl chains we have found the fascinating result that the double bonds in a diunsaturated fatty acid are very highly ordered, but interconvert rapidly between ordered states so as to give an appearance of disorder. This adds further insight into the valuable role played by polyunsaturated fatty acids in biological systems.

Tu-AM-D2 PHOSPHOLIPID/CHOLESTERYL ESTER/CHOLESTEROL/APOPROTEIN A1 MICROEMULSIONS: LIPID-PROTEIN MODEL SYSTEMS FOR HUMAN SERUM LIPOPROTEINS. Robert E. Reisinger, James A. Hamilton, and David Atkinson (Intr. by Mary T. Walsh). Biophysics Institute, Housman Medical Research Center, Boston University School of Medicine, Boston, MA 02118.

As models for the lipid-protein interactions in human serum lipoproteins, microemulsions (ME) of dimyristoyl phosphatidyl choline (DMPC), cholesteryl oleate (CO), and varying amounts of cholesterol (C), were prepared by sonication and ultracentrifugation. Human apoprotein A1 (apoA1) was incorporated by incubating ME with apoA1 for 16hr at room temperature. Gel filtration chromatography showed the components to coelute from Sepharose CL-4B, demonstrating the formation of a well defined ME containing apoA1. Incorporation of apoA1 occured at a weight ratio of 0.2 with respect to DMPC and was independent of C composition. The CO to DMPC ratio (~0.9 mol/mol) was unaffected by the addition of apoA1. By differential scanning calorimetry, ME without apoA1 exhibit a DMPC acyl chain thermal transition (~25°) and a CO liquid crystal to liquid transition (~40°). The DMPC transition broadens progressively as a function of increasing C concentration, with a loss of enthalpy; no significant changes are seen for the CO transition. With apoA1 on the particle at 10 mol % C, the CO transition also broadens, and overlaps the broadened DMPC transition. An additional thermal event is observed at ~80° resulting from the unfolding of apoA1 and disruption of the particle. ^{13}C-NMR spectroscopy of ME prepared with ^{13}C isotopically enriched Cs suggests that significantly less surface-located C is observed in the presence of apoA1. Thus, in the presence of apoA1, C appears to affect the core-located CO.

Tu-AM-D3 ELECTRON MICROSCOPY OF UNSTAINED FROZEN HYDRATED LOW DENSITY LIPOPROTEIN (LDL). David Atkinson (Intr. by D.M.Small), Biophysics Institute, University School of Medicine, Boston, MA 02118.

To investigate directly the structure and morphology of LDL, recent advances in electron microscopic imaging of unstained biological macromolecules in the frozen hydrated state have been utilized. Thin films of dilute LDL solution (.5mg prot/ml) formed on holey carbon grids were rapidly frozen by plunging into liquid ethane and examined in the electron microscope at -165°C. Under these conditions LDL is preserved in vitreous ice and may be imaged directly by phase contrast electron microscopy. In low dose images (~ 20 e/Å) from ice films 500-100Å thick, LDL was seen as a circular particle 220Å diameter. A low contrast 180Å diameter core region was seen clearly, surrounded by a high contrast shell, reflecting the core and surface location of the neutral lipid and protein/phospholipid head groups. Translational and rotational image alignment, averaging and Fourier filtering of two independent subsets of the images showed the surface of the particles to have a sub-structure which may reflect the organization of apoprotein B and phospholipid at the surface. In separate studies monoclonal antibodies to apoB bound to LDL could be visualized at the particle surface. More extensive averaging and processing techniques currently being applied to these images will provide a more detailed description of the structure of LDL and the organization of apoB at the particle surface.

Tu-AM-D4 ANTIBODY-MEMBRANE INTERACTION: BINDING, LATERAL DIFFUSION AND LATERAL SEGREGATION. Lukas K. Tamm (Intr. by John G. Nicholls) Biocenter, University of Basel, CH-4056 Basel, Switzerland

Binding of monoclonal anti-lipid hapten antibodies to lipid vesicles containing lipid hapten at various mole fractions was studied by fluorescence spectroscopy. Fitting the resulting binding isotherms to the classical Langmuir adsorption model led to highly inconsistent binding constants. However, fits to a statistical binding model taking into account the bivalency and the large size of the ligand, reproduced the same unique binding constant at all lipid hapten densities.

Lateral diffusion of membrane-bound antibodies was measured by fluorescence recovery after photobleaching on single planar bilayers which were supported on silicon wafers. The diffusion coefficient of the antibodies was one half of the lipid diffusion coefficient. The antibody diffusion coefficients decreased 3-fold when the antibody surface concentrations were increased from a very low value up to near saturation. A sharp chain melting transition was observed in supported DMPC bilayers and was upshifted by 3°C when antibody was bound. As visualized directly by fluorescence microscopy, bound antibodies segregated laterally and reversibly into distinct domains below the lipid chain melting phase transition temperature.

Tu-AM-D5 EFFECTS OF LIPID PACKING ON POLYMORPHIC PHASE BEHAVIOR AND MEMBRANE PROPERTIES. Sek Wen Hui and Arindam Sen. Department of Biophysics, Roswell Park Memorial Institute, Buffalo, New York 14263.

The self assembly of phospholipid molecules in bilayer and non-bilayer forms was considered in terms of equivalent molecular shapes representing intermolecular forces. The equivalent size of each phospholipid headgroup was derived from the net atomic volume plus the volume of the associated water molecules, which was derived from water/hydrocarbon partitioning experiments. The equivalent lengths of unsaturated acyl chains were derived from the retention time data from chromatographic measurements. The spontaneous curvature of various phospholipid monolayers were calculated, and the energy required to flatten them to the bilayer plane was determined, using known bending modulus. The bending energy is in the order of kT. The onsets of bilayer to H_{II} transitions in various mixtures of PC, PE, cholesterol and diacylglycerols occur when the bilayers attain the highest bending energy state. Under this condition, the mixtures showed maximal susceptibility to phospholipase A_2, facilitated lipid transfer rate by phospholipid-exchange-proteins, permeability to carboxyfluorescein, incorporation of human erythrocyte proteins, and calcium transport by Ca-ATPase from SR in reconstituted vesicles. When the calculation was applied to known lipid compositions of nine cellular membranes, the protein/lipid ratio and phospholipid/cholesterol ratio were found to have a positive and a negative correlation, respectively, with the bending energy of the phospholipids. The energy expense in conforming to a bilayer phase may be an important physical parameter regarding the activity and the biogenesis of membranes.

Tu-AM-D6 **Regulation of Protein Kinase C Activity by Lipid** Alexandra C. Newton* and Daniel E. Koshland†, Jr. *Chemistry Department, Indiana University, Bloomington, Indiana 47408 and †Biochemistry Department, University of California, Berkeley, California 94720.

The regulation of the Ca^{2+}/lipid-dependent protein kinase C by diacylglycerol and phospholipid is examined for autophosphorylation and for substrate phosphorylation. Because protein kinase C autophosphorylates by an intrapeptide reaction, this activity depends directly on the kinase:lipid interaction, thus allowing the effect of lipid on the intrinsic kinase activity to be determined. In contrast, substrate phosphorylation depends on the interaction of three distinct components (susbstrate, kinase, and lipid), so that activity reflects protein:protein as well as protein:lipid interactions. Examination of both modes of activity reveals that diacylglycerol directly activates protein kinase C while phospholipid exerts its regulatory action not only through its affects on protein kinase C, but also through its interaction with substrate. While the activation of protein kinase C by phospholipid is specific for phosphatidylserine, regulation of substrate phosphorylation is sensitive to membrane surface charge. Thus, lipid regulates protein kinase C activity in three ways: 1. diacylglycerol activates the enzyme, 2. phosphatidylserine regulates the degree of activity, and 3. membrane surface charge modulates substrate phosphorylation.

Tu-AM-D7 PROJECTED STRUCTURE OF Na,K-ATPASE CRYSTALS MAINTAINED IN VITREOUS ICE
M. MISRA, H. C. Beall, K. A. Taylor and H.P. Ting-Beall. Cell Biology Department, Duke University Medical Center, Durham, NC 27710

The detailed description of the mechanism of active transport of Na^+ and K^+ ions requires a molecular description of the Na,K-ATPase in the native state. To achieve this we have utilized electron microscopy of ordered arrays of Na,K-ATPase molecules produced by phospholipase A_2 and VO_3^- (Mohraz et al., J. Ultra. Res. 93, 17 (1985)) and preserved frozen-hydrated in amorphous ice. We used the technique of correlation averaging (Frank, et al., Ultramicroscopy 6, 343 (1981)) for image processing because of lattice disorder present in these crystals. Original images and averaged reconstructions of both negatively-stained and frozen-hydrated crystalline sheets reveal Na,K-ATPase dimers arranged in parallel rows of paired molecules with cell dimensions of a=14.7nm, b=5.2nm and γ=98°. The averaged images of these crystalline sheets reveal asymmetry between the two protomers in the dimer chain that has not been observed by other investigators. To check this observation, we processed images of negatively stained Ca^{2+}-ATPase crystals by the same correlation averaging procedure and calculated an averaged image of Na,K-ATPase crystals using the unbending procedure of Henderson et al. (Ultramicroscopy 19, 147 (1986)). Correlation averaging produced an image of symmetric dimers for the Ca^{2+}-ATPase crystals, in confirmation of earlier results by numerous investigators. Unbending produced an image of asymmetric dimers for the Na,K-ATPase. We also estimated the degree of asymmetry from (1) residuals after phase origin search for presumptive 2-fold axes and (2) by calculating transform power loss after symmetrization. The latter analysis was also done on a model Ca^{2+}-ATPase image with different degrees of added noise. Both phase residuals and transform power loss indicate a significantly greater asymmetry in the images of Na,K-ATPase than Ca^{2+}-ATPase. This dimer asymmetry could arise from of the simultaneous existence of two different forms of the enzyme. This research is supported by NIH Grants GM 27804 and GM 30598 and by an Established Investigatorship from the American Heart Association to (K.A.T.)

Tu-AM-D8 GAP JUNCTION TRANSMEMBRANE DOMAIN: SURVEY OF PLAUSIBLE STRUCTURES BY SIMULATED FIBER DIFFRACTION, Thomas T. Tibbitts, Donald L. D. Caspar, Walter C. Phillips, and Dan A. Goodenough+, Rosenstiel Basic Medical Sciences Research Center, Brandeis University and+ Department of Anatomy, Harvard Medical School.

Based on primary sequence analysis, an alpha helical folding of the polypeptide chains transversing the gap junction membrane has been proposed (see Hertzberg et. al. (1988) in Gap Junctions, eds. Hertzberg and Johnson; Milkes et. al. (1988), EMBO J. 7:2967). Secondary structural information is available in X-ray diffraction patterns from isolated plaques: a broad maxima on the equator (0.06 - 0.14 $Å^{-1}$) and a group of four fringes near the meridian centered at 0.21 $Å^{-1}$. We have simulated powder and fiber diffraction from alpha helices, beta sheets, and whole proteins representative of different structural types to interpret these data. All proteins studied show two maxima in their powder patterns near 0.09 $Å^{-1}$ and 0.22 $Å^{-1}$. The ratio of intensity in these peaks is characteristic of the protein tertiary class. Gap junction diffraction indicates a ratio closest to that of up-and-down helix bundle proteins. Similiarly, fiber patterns of different proteins show different strength intensity on the equator between 0.6 - 0.14 $Å^{-1}$, relative to that on the meridian between 0.18 - 0.24 $Å^{-1}$. This ratio is sensitive to the type of secondary structures present and their orientation to the fiber axis. Proteins which contain up-and-down alpha helix bundles oriented with one or more of the strands tilted between 25° and 55° give patterns most like gap junction diffraction patterns.

Tu-AM-D9 PROJECTED DENSITY OF THE VDAC CHANNEL: CORRELATION AVERAGING OF ELECTRON IMAGES OF FROZEN-HYDRATED MEMBRANE CRYSTALS. Carmen A. Mannella, Bernard Cognon. Wadworth Ctr. for Labs & Res., NYS Dept. of Hlth., Albany, NY 12201, and Dept. of Biomedical Sci., SUNY-Albany.

Two-dimensional crystals of the VDAC channel are formed by slow lipid depletion (using phospholipase A_2) of outer membranes isolated from Neurospora mitochondria. Electron microscopic images have been recorded from unstained channel arrays embedded in vitreous ice. Quasi-optical Fourier filtration provides a preliminary unit-cell average, which is subsequently cross-correlated with the entire crystalline field. Final averages are formed by summing areas windowed at the coordinates of peaks in the cross-correlation function (CCF). In general, fewer peaks are detectable in the CCFs of these low-contrast images compared with equivalent areas of negatively stained arrays; increasing defocus improves peak detection considerably. Correlation averages over 150-300 unit cells have apparent p2 symmetry. Best averages to date have effective resolution of approx 1/(2 nm) with weak maxima in Fourier power spectra out to 1/(1.5 nm). Unit cell dimensions (13.0 nm x 11.3 nm, θ = 108.5°) and arrangement of the six channels within the unit cell are the same as previously reported for negatively stained specimens. In frozen-hydrated averages, each channel projection appears as a low-density (water-filled) polygon, approx 2.5 nm across, bounded by a high-density (protein) rim. The rims are not uniform, but contain 3 or 4 maxima distributed asymmetrically around each lumen. Also, dense (protein) arms extend from the channels, appearing to bridge adjacent channel complexes. Minima in the density maps correlate well with loci of light staining by uranyl acetate in negatively stained arrays; these are likely phospholipid domains. (Supported by NSF grant DMB-8615666).

Tu-AM-D10 LOCALIZATION OF BINDING OF A POLYANION EFFECTOR TO THE VDAC CHANNEL BY CORRELATION ANALYSIS OF 2D CRYSTALS. X.-W. Guo, C.A. Mannella (Intr. by G.W. Brady). Wadsworth Ctr. for Labs & Res., NYS Dept. of Hlth., Albany, NY 12201, & Dept. of Physics, SUNY-Albany.

The VDAC channel of the mitochondrial outer membrane switches to lower conductance states in response to transmembrane potentials. Mangan and Colombini (PNAS 84:4896) report that a copolymer of methacrylate, maleate and styrene (1:2:3, MW 10,000) induces similar low-conductance states in VDAC and increases the voltage sensitivity of channels that remain open. We are using electron microscopy and image analysis to determine the structural basis for the effects of the polyanion (PA). Suspensions of 2D crystals of VDAC (formed by phospholipase A_2 treatment of Neurospora mitochondrial outer membranes) have been embedded in aurothioglucose at various times after addition of 5μM PA and electron images recorded. Optical diffraction and correlation analysis indicate three effects of increasing exposure to PA: (1) disordering of the normal VDAC parallelogram arrays and appearance of a contracted form of the array; (2) statistically significant decrease in projected diameters of the stain-filled channel lumens, from 2.5 to 1.7 nm; and (3) new narrow zones of stain exclusion around the channels. Since the latter features are never seen in the absence of PA, they probably represent predominant sites of PA binding. Mapping of these features to correlation averages of control, frozen-hydrated arrays indicates that PA (an amphiphilic polymer) binds at the protein/lipid boundary along the channel exterior. This binding may cause a conformational change in VDAC to a narrower lumen (effect #2) which might also alter channel packing (effect #1). Effect #2 could also be due to binding of PA along the channel lumen, excluding gold-glucose. (Supported by NSF grant DMB-8615666.)

Tu-AM-D11 **SELFORGANIZATION OF ION CHANNELS,** **Peter Fromherz, University Ulm, FRG.** The lateral distribution of membrane proteins and of the electrical membrane potential is studied in a theoretical model. The dynamics is described by a Smoluchowski equation with respect to lateral diffusion and drift of the proteins and by a Kelvin equation with respect to propagation and relaxation of the potential. These well-known partial differential equations are mutually coupled by a channel conductance and an electrophoretic charge of the mobile proteins. The coupling gives rise to spontaneous condensation in a fluid mosaic if the membrane is far from electrochemical equilibrium. Pattern formation is controlled by the gradients of ion concentration, by the density of charged channels, by the mobility of proteins and by the shape of membrane and electrolyte. These parameters correspond to biological features as to the activity of pumps, to the gating of channels, to interactions of the cell skeleton and to the growth of cells. The geometries of a finite free cable, a free sphere and a sphere near a surface are studied by linear stability analysis and numerical integration. Stationary, oscillatory and solitary waves are observed. This physical model of "morphogenesis" relies on mere transport across and along membranes. Chemical reactions are not involved directly. The ion channels and the potential play the role of "morphogens".
References: PNAS 85(1988)6353, BBA 944(1988)108

Tu-AM-D12 TRANSFECTION OF L FIBROBLASTS WITH L-SCP DNA ALTERS CELL GROWTH, LIPID COMPOSITION, AND MEMBRANE BIOPHYSICAL PROPERTIES. J.R. Jefferson*, D. Powell*, Z. Rymaszewski#, J. Kukowska-Latallo@, J.B. Lowe@ and F.Schroeder*+. *Depts., Pharm.& Med.Chem., Coll. of Pharmacy, +Pharm.& Cell Biophys., #Ophthalmology, Coll.of Med., Univ. of Cincinnati, Cincinnati, OH 45267; @Dept.Path.& Lab.Med. and Howard Hughes Med.Inst.,Univ. of Michigan, Ann Arbor, MI 48105.

It is proposed that the 15kD sterol carrier protein found in rat liver (L-SCP) is involved in determining the intracellular distribution of cholesterol and thereby membrane structure. The L-SCP gene was transfected into fibroblasts and high- and low-expression clones were isolated. A correlation was observed between expression of L-SCP and i) cell growth, ii) fatty acid and sterol composition, and iii) plasma, microsomal, and mitochondrial membrane physical properties. Clones expressing high levels of L-SCP had higher saturation density, acyl-CoA:cholesterol acyltransferase (ACAT) activity, and phospholipid unsaturated fatty acid ratio. The steady-state polarization, limiting anisotropy and fluorescence lifetime of diphenylhexatriene (DPH), as determined by multifrequency phase fluorometry in isolated plasma-membrane vesicles, was significantly lower in high-expression clones. These findings are consistent with the in vitro ability of L-SCP to stimulate ACAT activity, and preferentially bind unsaturated fatty acids and sterols. The biophysical results indicate a lower degree of membrane-lipid order, consistent with reduced membrane sterol and elevated unsaturated fatty acid levels. A plausible effect of higher concentrations of L-SCP would be a shift in the equilibrium partition of sterol towards the aqueous phase. (Supported by NIH grants GM 31651, F.S.; HL 07460, J.R.J.; DK 38482 J.B.L.)

Tu-AM-E1 H-BOND BREATHING MODES AND THE ENERGETICS OF RNA TRANSCRIPTION, E.W. Prohofsky, Department of Physics, Purdue University, W. Lafayette, IN

A theoretical study of double helical melting indicates that a group of vibrational modes, the H-bond breathing modes, are the principal initiators of helix melting. Many biological processes such as RNA transcription require that energy be supplied to the transcription complex. The energy requirement is principally necessary to melt base pairs so the complex can advance. Calculations indicate that the H-bond modes can both supply the needed energy and bring about the necessary base pair separation with amplitudes within the range occuring in thermal fluctuations. Nonlinear factors can improve the efficiency of this mechanism for achieving local energy conservation in these biological processes. Similar modes are found in RNA double helices and such modes are expected in double helical stretches in r. ibosomes and may play a role in translation.

Tu-AM-E2 UV RESONANCE RAMAN STUDIES OF PEPTIDE CONFORMATIONS AND AMIDE EXCITED STATES. Sunho Song and Sanford A. Asher, Department of Chemistry, University of Pittsburgh, Pittsburgh, Pennsylvania 15260, Samuel Krimm, Biophysics Division, University of Michigan, Ann Arbor, MI 48109.

We have examined the UV resonance Raman spectra of a series of small peptides and poly(L-glutamic acid) and poly(L-lysine) in their random coil, α-helix and β-sheet conformations. We assign the resonance enhanced amide bands, and characterize their resonance enhancement mechanisms. We observe strong enhancement of the amide II, III and II' bands via amide $\pi\rightarrow\pi^*$ electronic transitions. In addition, a strongly enhanced conformational sensitive band in the resonance Raman spectra of polypeptides and small model complexes between 1330 cm^{-1} - 1445 cm^{-1} in resonance with the amide $\pi\rightarrow\pi^*$ transition is assigned to the overtone of the amide V vibration. The amide V band derives from C-N torsion and N-H out-of-plane bending, and is weak in Raman but strong in IR. We also assign an enhanced 1496 cm^{-1} band of N-methylacetamide with 220 nm excitation, which is not observed in normal Raman spectra, to the overtone of amide V. The unique enhancement of the amide V overtone bands indicate that the π^* state is twisted relative to the ground state. We have examined the pH and conformational dependence of the amide band frequencies and Raman cross sections and relate these dependences to changes in the resonant electronic transition frequency and oscillator strength. The intensities of the overtone of amide V as well as the amide II and III bands show a correlation to protein conformations in the UV resonance Raman spectroscopy. We have used these amide band frequencies and intensities to monitor the conformation of peptides and proteins and have examined the temperature and pH dependences of poly(L-lysine) conformation.

Tu-AM-E3 UV RESONANCE RAMAN ENHANCEMENT OF THE VINYL STRETCH IN FERRIC PROTOPORPHYRIN-IX: CONJUGATION OR PRESERVATION OF THE VINYL $\pi\rightarrow\pi^*$ TRANSITION?
Valentino L. DeVito and Sanford A. Asher, Department of Chemistry, University of Pittsburgh, Pittsburgh, Pennsylvania 15260.

Ultraviolet resonance Raman spectra of several ferric protoporphyrin-IX complexes are presented. These include the five-coordinate high spin μ-oxo dimer $(FePP)_2O$, and the six-coordinate low spin bis-liganded porphyrin complexes of imidazole (ImH) and cyanide, $[(ImH)_2Fe(PP)]^+$ and $[(CN)_2Fe(PP)]^-$. Excitation in the 220-275 nm region results in selective enhancement of the vinyl C=C stretching mode at 1622 cm^{-1}. This enhancement derives from a transition at ca. 200 nm and indicates the existence of an almost isolated vinyl $\pi\rightarrow\pi^*$ transition. From comparisons between the Raman spectra of protoporphyrin-IX complexes and 1-hexene and 1,3-hexadiene, we assess the extent of π-conjugation of the vinyl-heme complex. We conclude that little conjugation occurs in the ground state. Our data suggest that resonance enhancement of this vibrational mode with visible Soret excitation derives from a large conjugation between the vinyl π^* antibonding orbitals with the porphyrin excited Soret state. Our data show the existence of a nearly independent vinyl $\pi\rightarrow\pi^*$ electronic transition in the UV absorption spectrum of porphyrins.

Tu-AM-E4 TRYPTOPHAN QUANTITATIVE UV-RESONANCE RAMAN EXCITATION PROFILES. Joyce A. Sweeney and Sanford A. Asher, Department of Chemistry, University of Pittsburgh, Pittsburgh, Pennsylvania 15260.

We have measured tryptophan total differential resonance Raman cross section excitation profiles for the 760, 1006, 1360 and 1550 cm^{-1} symmetric vibrational modes between 207 and 250 nm. These excitation profiles specify the optimum excitation wavelength for selective enhancement of tryptophan residues in UV resonance Raman (UVRR) studies of protein. Tryptophan shows saturation phenomena at the incident energy fluxes delivered by typical 20 Hz Nd-YAG laser-based excitation sources. Saturation manifests itself as a reduction in Raman intensity due to the depletion of ground-state tryptophan molecules by molecular absorption to the excited $B_{a,b}$ state with subsequent relaxation to the long-lived L_b excited state. The L_b excited state, which is the lowest lying excited singlet state of tryptophan, creates a bottleneck for relaxation back to the ground electronic state. Methods previously developed in our laboratory, which involve linear extrapolation to zero incident energy flux, eliminate the effect of saturation on excitation profile measurements. We also employed a 200 Hz XeCl excimer laser for excitation wavelengths between 207 and 214 nm. The longer pulse width (16 ns versus 6 ns for the Nd-YAG laser) and the higher repetition rate of the excimer laser result in high S/N ratios without saturation. The resonance Raman excitation profile (RREP) maxima for the tryptophan vibrational bands at 760, 1006, 1360 and 1550 cm^{-1}, occur at 224 nm, 4 nm red-shifted from the absorption maximum of the $B_{a,b}$ electronic transition. This red-shift may derive from destructive interference by the electronic transition showing an absorption maximum at 195 nm. We used Resonance Raman Transform Theory to investigate the influence of this electronic transition on the vibrational bands studied.

Tu-AM-E5 THE *TRANSITION LYING BETWEEN THE $n-\pi^{*}$ AND $\pi-\pi^{*}$ OF ALIPHATIC DIKETOPIPERAZINES IS AN $n-\sigma^{*}$. Wilson Radding, sponsored by Richard Shoemaker, Department of Physiology and Biophysics, UAB, Birmingham, AL 35294.

Most absorption and circular dichroism studies of peptides assume that there are only two transitions below 190nm, the $n-\pi^{*}$ and the $\pi-\pi^{*}$. Circular dichroism studies of diketopiperazines show unequivocally that there is another transition which generally lies between the two. Absorption and circular dichroism spectra were performed in solvents of varying hydrogen bonding capability at room temperature and at liquid nitrogen temperature. The wavelength of this second lowest energy band is sensitive to both the hydrogen bonding capability of the solvent and the ambient temperature in a manner which is consistent with only one of the possible transition types, the $n-\sigma^{*}$.

Tu-AM-E6 PHOSPHORESCENCE AND OPTICALLY DETECTED MAGNETIC RESONANCE STUDIES OF ECHINOMYCIN-NUCLEIC ACID COMPLEXES. T. Alfredson and A.H. Maki, Department of Chemistry, University of California, Davis, CA 95616.

Spectroscopic investigations of echinomycin, a bis-intercalating quinoxaline antibiotic, and echinomycin-nucleic acid complexes have been carried out in order to provide insights into the role of stacking interactions of the drug's quinoxaline moieties upon binding to nucleic acid targets. We have utilized phosphorescence and optically detected magnetic resonance (ODMR) to yield information on the environmental perturbations of the quinoxaline residues in the drug upon complexation with natural and synthetic nucleic acids.

X-ray crystallographic studies[1] using model oligonucleotides have demonstrated DNA minor groove binding of echinomycin with the quinoxaline residues bis-intercalating two dC-dG steps. By means of footprinting techniques[2] the drug has been shown to have a binding preference for G+C rich nucleic acids. Results of ODMR studies which reveal changes in the quinoxaline probe environment upon drug binding to nucleic acid targets will be presented. Slow passage ODMR measurements of the zero field splittings indicate differences in quinoxaline stacking interactions with M.Lysodeikticus DNA compared with interactions taking place in complexes with poly(dG·dC) and poly(dG)·poly(dC). Further results bearing on the dynamics of the quinoxaline triplet state will be presented.

1. Wang, A.H., Ughetto, G., Quigley, G.J., Hakoshima, T., van der Marel, G.A., van Boom, J.N. and Rich, A. (1984) Science, 225, 1115-1121.
2. Low, C.M., Drew, H.R., and Waring, M.J. (1984) Nucleic Acids Res., 12, 4865-4879.

Tu-AM-E7 Is The Active Site Of Monoamine Oxidase A Identical To Monoamine Oxidase B ? A Spin Label Study.

Henry M. Zeidan, Sulivanus Oyouga and William Dashek
Atlanta University, Chemistry Department and Biology Department
Atlanta, Georgia 30314.

The Spin Labeled substrate , tryptamine, was used as a structural probe of the active site of rat brain Monoamine Oxidase A. When the reaction was monitored by electron spin resonance(ESR), line broadening effects indicative of binding with an apparent relation to substrate specificity for the enzyme was observed. The spectrum indicated that the bound label was partially immobilized with a dissociation constant of 42 M and 2.4 mole per enzyme dimer. The correlation time, reflecting the environment of the tryptamine binding site , was determined to be 5.2 sec. MAO A from rat brain appears to be sensitive to trypsin hydrolysis, while MAO B is insensitive. Recent investigations by this laboratory and the present study suggest that the structure of rat brain MAO A is close but not identical to MAO B.

[This work was supported by NIH Grant # RR08247 and NIH RCMI Grant # 1 G 12-RR-03062].

Tu-AM-E8 FLUORESCENCE ENERGY TRANSFER DETECTS CHANGES IN FIBRONECTIN STRUCTURE UPON SURFACE BINDING. C. Wolff, C. Narasimhan, and C.-S. Lai, National Biomedical ESR Center, Medical College of Wisconsin, 8701 Watertown Plank Road, Milwaukee, Wisconsin 53226.

Plasma fibronectin (Fn), a glycoprotein found in blood plasma, comprises two multifunctional subunits joined by two disulfides at their carboxyl termini. The protein participates in many processes including cell adhesion and spreading, and wound healing. Most of these functions are expressed when Fn is immobilized on a surface and have been attributed to the surface activation of the Fn molecule. This study attempts to explore the molecular nature of this activation process.

Fn contains two free sulfhydryl groups per chain; one located between the DNA-binding and cell-binding domains (SH_1) and the second situated in the carboxyl terminal fibrin-binding domain (SH_2). Recently, we have succeeded in selectively labeling one out of the two sulfhydryls per chain. The sulfhydryls near the cell-binding domains were labeled with coumarinylphenylmaleimide (CPM) and the glutamine-3 residues, near the amino terminus of each chain, were labeled with monofluoresceinyl-cadaverine, using coagulation factor $XIII_a$. Emission spectra of the double-labeled protein in solution showed the occurence of energy transfer, indicating that the two regions are within 70 A. Upon surface binding to dextran microcarriers a decrease in the energy transfer was detected.

Moreover, Fn labeled at SH_1 with CPM and subsequently at SH_2 with fluorescein-5-maleimide, showed a small amount of energy transfer in solution, indicating that these sites may also be within 70 A of each other. Distances between the sulfhydryls and between each sulfhydryl and the amino termini, as well as changes observed upon surface binding will be presented. The results are consistent with the notion that Fn undergoes a conformational change upon surface binding, which may be important in the surface activation process of the Fn molecule.

Tu-AM-E9 **FLUORESCENCE STUDIES ON MELANIN STRUCTURE.** C. Pande*, T. Schultz. Clairol Research Laboratories, Stamford, CT. 06922.

Melanin is a generic term used for all black pigments produced in animals and plants by oxidative polymerization of catechol-type monomers. Eumelanin, the black pigment found in human hair and skin and in the ink-sacs of the cuttlefish *(sepia)*, results from enzymatic oxidation of tyrosine. The reaction is believed to involve the formation of 3,4-dihydroxyphenylalanine (DOPA), cyclization of DOPA to melanin precursers such as 5,6-dihydroxyindole-2-carboxylic acid (DHICA) and 5,6-dihydroxyindole (DHI), followed by polymerization of these molecules. The natural pigment is formed as a protein complex in vivo. Despite their ubiquitous presence, the structure(s) and function(s) of melanins remain elusive and not well understood.

The absorption spectra of melanins do not show any chromophoric absorption band. Instead, the absorbance increases monotonically with decreasing wavelength, somewhat analogous to the absorption of amorphous semiconductors. Thus, this technique is not likely to be structure sensitive, at least in the case of natural melanin.

We have recently initiated detailed fluorescence studies on melanins. In contrast to the absorption results, preliminary studies clearly reveal the presence of multiple fluorophores in the solubilized form of both natural *(sepia)* and synthetic DHI melanin. Furthermore, the wavelengths of the emission maxima are significantly different for the two melanins. Thus, unlike absorption, fluorescence appears to be much more structure sensitive. Experiments are underway to characterize the units (fluorophores) responsible for the observed fluorescence. These experiments include studies on the model systems considered to be likely fluorophores in the two melanins. Results from these studies will allow translation of the fluorescence excitation and emission spectral information into structural details.

Tu-AM-E10 STRUCTURE, ENVIRONMENT AND FLUORESCENCE OF PRODAN.

Predrag Ilich, Paul H. Axelsen and Franklyn G. Prendergast,
Department of Biochemistry and Molecular Biology, Mayo Foundation, Rochester, Minnesota 55905.

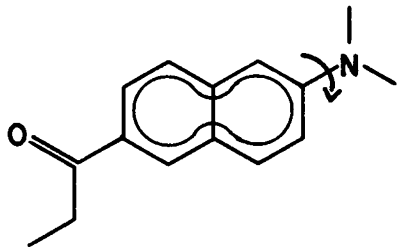

INDO/S electronic structure calculations require that a good fluorophore has (a) an aromatic ring, providing π-electrons of low energy and high state symmetry, (b) diametrically positioned substituents, enabling a low energy biallylic structure of excited state, and (c) different local charge densities on substituent groups, enabling intramolecular charge separation in low singlet excited states. Intermolecular effects, evaluated through one-electron terms, indicate that color and intensity of emission may be ultimately determined by (d) embedding restrictions on a terminal amino group (Figure), and (e) availability of highly charged groups in the substituents' proximity. These requirements were evaluated in the case of 6-acryloyl-2-(dimethyl)aminonaphthalene, ACRYLODAN [F.G. Prendergast et al. (1983) J. Mol. Biol. 258, 3868)], covalently bound to carbonic anhydrase and to cystein proteinases, papain and actinidin. The theoretical results appear to largely corroborate experimental spectroscopic data. Supported by grant GM34847.

Tu-AM-E11 **QUANTITATION OF INTRACELLULAR [Ca^{2+}] FROM SPECTRA OF INDO-1 AND FURA-2 DYES.**

Charles S. Owen, Dept of Biochemistry, Jefferson Medical College, Philadelphia, PA

The use of the spectral shift in Indo-1 or Fura-2 to measure intracellular calcium ion activity requires knowledge of the spectra of the dye before and after chelation of a calcium ion. However, for both dyes, intracellular spectra differ from the analogous spectra measured in buffer. Calcium-free Indo-1 spectra, in particular, showed very different peaks inside and outside cells. This may be due to a reaction of dye with a component of the intracellular milieu, since: (1) a mathematical analysis showed that the new peak was not a composite of calcium-bound and free forms, such as would arise from residual intracellular calcium, and (2) the reaction was reversible upon dilution by sonication. In order to generate a consistent model for the intracellular chemistry of Indo-1 and Fura-2, it was assumed that the two enter into essentially the same intracellular reactions. The extra reaction appeared not to be strictly competitive with calcium binding. When the intracellular dye spectra for calcium-bound and unbound dye were used in data analysis, the calculated $[Ca^{2+}]_i$ was the same for both Indo-1 and Fura-2. The value agreed with the 100 nM value found in single permeabilized cells if the effect of the "extra" binding reaction on the apparent K_d for calcium was to increase K_d by a factor of 2.5.

Tu-AM-E12 HETEROGENEITY OF BENZO(A)PYRENE DIOL EPOXIDE-DNA BINDING AS PROBED BY FLUORESCENCE VIBRONIC INTENSITIES. H.C. Brenner, S.K. Kim and N.E. Geacintov, Department of Chemistry, New York University, New York, NY 10003

Covalent binding of the (+) and (-) enantiomers of anti-7,8-dihydroxy-9,10-epoxy-benzo(a)pyrene (BPDE) to DNA produces differing distributions of chemical adducts, as well as a different distribution of physical conformations (e.g. intercalative vs. solvent exposed). The distinct DNA binding properties of these enantiomers, which is believed to be related to their contrasting biological activities, can be probed by the fluorescence vibronic intensities of the pyrenyl residue at the DNA binding site, which in the parent hydrocarbon, are well known to be sensitive to the polarity of the environment. In particular, polar solvents, by effectively breaking the molecular symmetry, cause an enhancement of the (0,0) fluorescence relative to the vibronic bands at longer wavelengths. In the BPDE-DNA adducts, and in the BP tetraol, the fluorescence and absorption bands are red shifted relative to pyrene by the mesomeric effect of the extended carbon skeleton, but the vibronic intensities retain their sensitivity to environmental polarity. The ratio of the intensity of band V at 399 nm to the (0,0) at 379 nm is significantly larger in the (-)-BPDE-DNA complex than in (+)-BPDE-DNA, and this is consistent with the previously demonstrated predominance of quasi-intercalative binding in this complex. At 77K, spectral resolution is enhanced, and a shift in the excitation wavelength of the (-)-BPDE adduct from 345 to 353 nm produces a 5 - 6 nm shift in fluorescence, and very dramatic changes in vibronic intensities. Application of the synchronous scanning fluorescence technique, in which excitation and emission monochromators are simultaneously scanned at a fixed wavelength offset, yields a clean resolution of the two major types of sites in this adduct.

Tu-AM-F1 SUBCELLULAR DYNAMICS OF $[Ca^{2+}]_i$ MONITORED WITH LASER SCANNED CONFOCAL MICROSCOPY IN A SINGLE VOLTAGE-CLAMPED VERTEBRATE NEURON.

Arturo Hernandez-Cruz, Francisco Sala and Paul R. Adams. (Intr. by M. V. L. Bennett). Howard Hughes Medical Institute. Dept. Neurobiology and Behavior, SUNY , Stony Brook, N.Y. 11794

We have combined laser scanned confocal microscopy and digital image processing to monitor spatiotemporal $[Ca^{2+}]_i$ gradients in optical slices of individual cells using Fluo-3, a new fluorescent Ca-indicator (R.Y. Tsien & A. Minta J. Cell.Biol. 105: 89a). Bullfrog sympathetic neurons were patch-clamped in the whole-cell mode and the free acid dye was applied through the pipette. Ca-currents were recorded in Ringer containing 2 mM $CaCl_2$, and 1 uM TTX. Dye calibration gave an apparent Kd for Ca^{2+} of 350 nM in the internal pipette solution (90 mM CsCl, 20 mM TEA, 5 mM HEPES ,1 mM Mg-ATP, 100 uM EGTA and 100 uM Fluo-3 ; pH 7.1). Resting Ca concentration was estimated as 50 nM, and Ca transients up to 300 nM were observed following a single 100 msec pulse, producing maximal inward current (~ 4 nA). High spatial resolution (~ 0.3 um) of Ca gradients in the entire optical slice required 1 sec scan duration. Hence, rapidly dissipating gradients could not be seen simultaneously in all regions of the cell. However, slow transients and steady-state subcellular Ca-gradients were clearly revealed. Images obtained by line-scanning the cell at a fixed position were more informative since millisecond-range temporal resolution and high spatial resolution across the cell were simultaneously achieved. Following the clamp pulse, there is an inward decrementing wave of increased Ca^{2+} which reaches the center of the cell in about 350 msec, however, the nuclear region shows an unexpectedly large signal, perhaps as a result of Ca^{2+} release near or within this structure. An increased $[Ca^{2+}]_i$ in the nucleus following the application of 10 mM Caffeine support this conclusion . Return of cytosolic $[Ca^{2+}]$ to resting levels takes place in few seconds, but nucleus gradients dissipate more slowly. We are comparing these results with spherical diffusion models that take into account buffering, release, pumping, and spatial inhomogeneities.

F. Sala supported by Fundacion Juan March (Spain).

Tu-AM-F2 INHIBITORS OF INOSITOL 1,4,5-TRISPHOSPHATE-INDUCED Ca^{2+} RELEASE FROM BRAIN MICROSOMES.

P. Palade, C. Dettbarn and P. Volpe. Department of Physiology and Biophysics, University of Texas Medical Branch, Galveston, Texas 77550.

Ca^{2+} release from isolated canine brain microsomes in response to additions of inositol 1,4,5-trisphosphate (IP_3) has been investigated by spectrophotometric assay using antipyrylazo III. Microsomes were prepared according to Edelman et al. (J. Neurosci. 5, 2609, 1985) and loaded with Ca^{2+} in a medium containing 40 mM KCl, 62.5 mM K-phosphate, 1 mM MgATP, 5 mM Na_2 phosphocreatine, 20 µg/ml CPK, 0.25 mM antipyrylazo III, 8 mM MOPS, pH 7.0. Many K^+ channel blockers (including a series of tetraalkylammonium and alkyltrimethylammonium ions, Ba^{2+}, 4-aminopyridine and quinine) inhibit IP_3-induced Ca^{2+} release, which is also greatly decreased by substitution of K^+ in the medium. Nevertheless, valinomycin is unable to restore releases in the presence of K^+ channel blockers. This suggests that counterion K^+ movement is necessary for IP_3-induced Ca^{2+} release but that its inhibition is not the mechanism of action of K^+ channel blockers in this system. We have also determined that heparin, phytic acid, cinnarizine, neomycin, Zn^{2+}, 9-aminoacridine, Cd^{2+}, TMB-8 and certain local anesthetics are effective inhibitors of IP_3-induced Ca^{2+} release, that dantrolene, nifedipine and dithiothreitol are not, and that ruthenium red is effective only at very high concentrations. These same brain microsomes also appear capable of producing a ruthenium red-insensitive caffeine-induced Ca^{2+} release in the presence of vanadate.

Supported by GM40068.

Tu-AM-F3 THEORETICAL AND EXPERIMENTAL STUDIES ON CROSSBRIDGE MIGRATION DURING CELL DISAGGREGATION

Aydin Tozeren, Kuo-Li Paul Sung and Shu Chien, Department of Mechanical Engineering, The Catholic University of America, Washington, DC 20064 and Department of Physiology and Cellular Biophysics, College of Physicians and Surgeons, Columbia University, New York, NY 10032

A micromanipulation method is used to determine the adhesive energy density (γ) between pairs of cytotoxic T-cells (F1) and their target cells (JY: HLA-A2-B7-DR4,W6). γ is defined as the energy per unit area that must be supplied to reduce the region of contact between a conjugated cell pair. Our analysis of the data indicates that the force applied by the micropipette on the cell is not uniformly distributed throughout the contact region as we had previously assumed (Sung et al., Science, 234:1405-1408, 1986), but acts only at the edges of the contact region. We show that γ is not constant during peeling, but increases with decreasing contact area of the conjugated cell pairs F1-JY, F1-F1 and JY-JY in contrast to the constancy of γ for typical engineering adhesives. This finding supports the notion that the crosslinking protein molecules slide towards the conjugated area across the leading edge of the separation while remaining attached to both cells. Our mathematical analysis shows that the elastic energy stored in the crosslinks by the membrane tensions balances the diffusive forces that act against crossbridge migration. The binding affinity between F1-JY is found to be approximately fifteen to twenty times larger than the corresponding affinity for F1-F1. The number of binding sites of F1 for attachment to JY is approximately the same for binding F1 to another F1 and vary between 10^5 and 10^6.

Tu-AM-F4 ARACHIDONIC ACID UNCOUPLES CARDIAC MYOCYTES. Janis M. Burt and David C. Spray. Department of Physiology, University of Arizona, Tucson, AZ and Department of Neuroscience, Albert Einstein College of Medicine, Bronx, NY.

Using dual whole-cell voltage clamp and dye injection techniques, arachidonc acid (AA) was found to reversibly uncouple neonatal rat cardiac myocytes in a dose and time dependent manner, 5 μM typically reducing coupling to immeasureable levels within 5-7 minutes. After pretreatment with 1 mM phenidone, an inhibitor of the AA metabolic cascade, the dose and time dependence of uncoupling was shifted to higher doses and/or longer exposure times. This protective action of phenidone was more dramatic when extracellular calcium was low (no added Ca, 0.5 mM EGTA). Pretreatment with ibuprofen or indomethacin, inhibitors of the cyclooxygenase portion of the AA metabolic cascade, did not protect against uncoupling by AA. Since the AA metabolic cascade is stimulated during ischemic injury of the heart, the role of this cascade in mediating the closure of the channel that occurs during healing over (following injury) was examined. Following injury to one cell of a pair of cells, the time course for healing over (monitored by voltage clamp) was significantly prolonged by phenidone pretreatment of the cells: without phenidone pretreatment healing over required 54 ± 4 seconds (SD,n=4), with phenidone pretreatment (60-90 minutes), 115 or 175 seconds (n=2) were required. These data are consistent with arachidonic acid mediating closure of the gap junction channel via two mechanisms: through activation of the lipoxygenase portion of the AA cascade (which may be calcium sensitive) and through direct action (calcium insensitive) on the channel protein, probably at the lipid-channel interface. Supported by: PHS grants HL31008 to JMB and HL38449 to DCS.

Tu-AM-F5 CYTOSKELETAL MODULATION OF EARLY ANTIPROLIFERATIVE SIGNALS OF ALPHA INTERFERON. A. Aszalos, E. Balint and P.M. Grimley, Food and Drug Administration, Washington, D.C. and Uniformed Services of the Health Sciences, Bethesda, MD. (Intr. by Ira Levin)

We established earlier that changes in K^+ fluxes and surface membrane receptor mobility are early events in the antiproliferative signaling of alpha interferon (IFα). These early changes occur only in Daudi cells sensitive to the antiproliferativ action of IFα, but not in insensitive, resistant subclones (Aszalos et al. Biophys. J. 53:352,1988; Balint et al. Scanning Microscopy, in press). We recently investigated the involvement of the cytoskeletal elements in these early events of the antiproliferativ signal of IFα . We found that depolimerization (colcemid, colchisine) or stabilization (D_2O, taxol) of the microtubulesystem (Aszalos et al.J. Cell Biol. 100:1857,1985) does not affect the early antiproliferativ events. However, treatment of the sensitive Daudi cells with cytochalasin B (10 ug/mL), the microfilament-affecting agent, modulates the IFα binding-induced K^+ flux and receptor mobility changes. Our results correlate well with Pfeffer's cosolubilization studies on IFα receptors and microfilaments (Pfeffer et al. Proc. Natl. Acad. Sci. 84:3249,1987). (Supported in part by USUHS MAALT project GM-74 AQ)

Tu-AM-F6 PATCH-CLAMP CAPACITANCE MEASUREMENTS REVEAL THE DYNAMICS OF EXOCYTOSIS IN SINGLE NEUTROPHILS

Oliver Nüße and Manfred Lindau
Biophysics Group, Dept. Physics, Freie Universität Berlin, D-1000 Berlin, FRG

The area of the plasma membrane increases when secretory granules fuse with this membrane during exocytosis. Since biological membranes have a remarkably constant specific capacitance of about 1 $\mu F/cm^2$ the membrane capacitance increases proportional to the membrane area. We have investigated the dynamics of granule fusion by time-resolved patch-clamp capacitance measurements in human neutrophils. Resting neutrophils had a membrane capacitance of 2.96 ± 0.13 pF. Including 20 μM GTP-γ-S in the intracellular (pipette) solution led to an increase of the capacitance to a final value of about 8.5 pF. During exocytosis capacitance steps of 1-10 fF were detected. The step size distribution is in good agreement with the size distribution of primary granules ($d=280 \pm 40$ nm). The secondary granules are too small to be resolved as discrete capacitance steps. The total amplitude is very close to the value expected for complete degranulation of primary and secondary granules. The amplitude is not affected by the intracellular free calcium concentration between 10 nM and 4 μM and by pretreatment with cytochalasin B. Both factors, however, modulate the time course of degranulation. The intracellular ATP concentration affects time course and amplitude of exocytosis. Maximal degranulation requires mM ATP.
This work was supported by the DFG, Sfb 312 / B6.

Tu-AM-F7 VOLTAGE DEPENDENCE AND ANTIBODY SENSITIVITY OF LENS CHANNELS ACROSS RECONSTITUTED SINGLE MEMBRANES AND JUNCTIONS BETWEEN TWO MEMBRANES. Gregory J. Brewer, L.J. Takemoto*, K.L. Draper and Ren-Jie Dong, Dept. Medical Microbiology & Immunology, Southern Illinois Univ. Sch. Med., Springfield, IL, *Dept. Biology, Kansas State Univ., Lawrence, KS.

To study the single channel activity in single membranes and in the adhesive junction between two membranes, spherical model membranes were reconstituted from 1-oleoyl-2-palmitoyl phosphatidylcholine and lyophilized bovine lens membranes. The conductance between two adhering membranes increases with the second power of the input protein concentration, suggesting that the rate of channel formation is dependent on the interaction of two components. With voltage clamped on each membrane, discrete current steps are observed in single membranes and across the junction between two membranes. In physiological saline, the mean single channel conductance of single membranes was 265 pS, independent of voltage. Across the junction, the mean single channel conductance was well described by a single exponential in voltage which was asymptotic at 75 pS for voltages above 25 mV. The extrapolated single channel conductance at 0 mV was 732 pS. An affinity purified polyclonal antibody to a C-terminal peptide of MIP26, the major intrinsic protein of lens membranes, was included inside one membrane. This condition resulted in significant reductions in the mean channel size both in the single membrane and across the junction. A control antibody against α-crystallin did not produce this effect. These results suggest that MIP26 forms voltage-dependent channels whose conductance is regulated differently in a single membrane and a junction between two membranes. Supported by NIH EY06077.

Tu-AM-F8 HOMO- AND HETEROTYPIC GAP JUNCTIONS BETWEEN CARDIAC MYOBLASTS AND FIBROBLASTS: DIFFERENCE IN SINGLE CHANNEL PROPERTIES. H.J. Jongsma, M.B. Rook, A.C.G. van Ginneken and B. de Jonge. Dept. of Physiology, University of Amsterdam, Meibergdreef 15, 1105 AZ, Amsterdam.
After enzymatic dissociation of neonatal rat hearts, pairs of myoblasts (MM), pairs consisting of a myoblast and a fibroblast (MF) and pairs of fibroblasts (FF) readily form in cell culture. Between these cell pairs gap junctions have been shown to be present, using electron microscopy. To obtain information about the conductivity of these gap junctions a double whole cell recording system was used, with a patch pipette Gigaohm sealed to each cell of a pair. In current clamp mode we recorded synchroneous action potentials from MM pairs. The delay between the actionpotentials depended on the degree of coupling. In MF pairs stimulation of the fibroblast by injection of depolarizing current pulses, elicited actionpotentials in the myoblast while in turn these actionpotentials resulted in passive depolarizations of the fibroblast. In FF pairs stimulation of one cell resulted in a transient depolarization which was electrotonically conducted to the other cell. In voltage clamp experiments on loosely coupled cell pairs we were able to record single gap junctional channel currents in all three cases. From the results we constructed frequency histograms of the single channel conductances. In the MM pairs we found conductance peaks at 18 and 48 pS. In the FF pairs a single peak at 21 pS was found while in MF pairs a single peak at the exact intermediate conductance - 29 pS - was found. From these results we conclude that connexons (hemichannels) of different cell types from the same organ have indentical extracellular domains and that the cell specific conductance of the connexons is brought about by either the intramembrane domain or the intercellular domain.

Tu-AM-F9 1-OCTANOL REDUCES CALCIUM, POTASSIUM AND GAP JUNCTIONAL CURRENTS IN MOUSE PANCREATIC BETA CELLS. Perez-Armendariz, E.M., Spray, D.C. and Bennett, M.V.L. Albert Einstein College of Medicine. Bronx, NY. 10461

Modulation of junctional conductance has been correlated with changes in secretory state of pancreatic beta cells. We have evaluated the effect of 1-octanol, an agent widely used to reduce conductance of gap junctions, on junctional and non-junctional currents in pairs of beta cells, which are electrically coupled (1). The patch pipette solution used to record outward and junctional currents contained (in mM): K-aspartate 100, KCl 35, KOH 20, EGTA 5.5, $CaCl_2$ 0.5, Mg-ATP 2, Na-ATP 3, and Hepes 5, pH 7.16. Calcium currents were recorded in a 10 mM $CaCl_2$, 5 μM TTX, Krebs-Ringer solution with a pipette solution containing (in mM): CsCl 130, CsOH 20, EGTA 10, $CaCl_2$ 0.5, Mg-ATP 2, Na-ATP 3, CPK 10, CP 50 U/ml, and Hepes 10, pH 7.16. In 8 pairs of beta cells, 2 mM octanol reduced junctional conductance, g_j, to unmeasurable levels within seconds; g_j, partially recovered within 1-2 min. In 6 cells, 1 mM 1-octanol reduced voltage-dependent potassium currents by 90% within seconds. The same concentration of octanol supressed voltage-sensitive calcium currents in 5 cells by at least 50% in the same period of time. Both currents completely recovered within one minute. Simultaneous monitoring of nonjunctional and junctional currents showed that reduction of j_g required the same or higher concentration of octanol than the reduction of potassium and calcium currents. Since sustained glucose-induced insulin release is dependent on calcium influx through voltage-sensitive channels, these findings indicate that octanol is not an appropriate uncoupling agent to evaluate the role of gap junctions in insulin release.

1) Perez-Armendariz, E.M., Spray, D.C. and Bennett, M.V.L. 1988. Bioph. J., 53:53a.

Tu-AM-F10 FORMATION OF HYBRID CELL-CELL CHANNELS. E. Levine, R. Werner, G.P. Dahl, Depts. of Physiology and Biophysics and of Biochemistry, University of Miami, Florida 33101.

The oocyte cell-cell channel assay (Dahl et al. 1987) was used to test the connexin-43 cDNA clone (Beyer et al. 1987) for its ability to direct the formation of cell-cell channels. Junctional conductances in oocyte pairs injected with mRNA synthesized in vitro from the connexin-43 cDNA clone are on the average 20 times higher than in non-injected control pairs. An increase in junctional conductance, although less pronounced, is also observed in pairs in which only one oocyte had been injected. The gating properties of channels formed in the latter strongly argue for the formation of hybrid cell-cell channels between connexin-43 channels and the oocytes' endogenous channels. Such channels respond to transjunctional voltage in an asymmetric fashion, whereas symmetric oocyte pairs (either injected or uninjected) have symmetric gating properties. Pure connexin-43 channels are not voltage gated, pure oocyte channels are voltage dependent, and the channels formed from oocyte and connexin-43 hemichannels have properties apparently contributed by both types of hemichannels. These hybrid channels rectify. They close in the same way as pure oocyte channels when the side containing the oocyte hemichannel faces the positive pole of the transjunctional voltage field, but when the field is reversed the channels remain open. These hybrid channels can serve as a model for the rectifying electrical synapses found between neurons. Supported by NSF (DCB-8605510)

Tu-AM-G1 TRANS-MEMBRANE ORIENTATION OF THE CHLOROPLAST CYTOCHROME b-559 psbE GENE PRODUCT.
G.-S. Tae, M. T. Black, and W. A. Cramer (Intr. by S. E. Ostroy), Department of Biological Sciences, Purdue University, West Lafayette, IN, 47907.

Protease accessibility and antibody to a COOH-terminal peptide were used as probes for the *in situ* topography of the M_r 10,000 psbE gene product (α subunit) of the chloroplast cytochrome b-559. Exposure of thylakoid membranes to trypsin or S. aureus V8 protease cleaved the α subunit to a slightly smaller polypeptide, as detected on Western blots, without loss of reactivity to COOH-terminal antibody. The disappearance of the parent M_r 10,000 polypeptide from thylakoids in the presence of trypsin correlated with the appearance of the smaller polypeptide with ΔM_r = -750, the conversion having a half-time of approximately 15 min. Exposure of inside-out vesicles to trypsin resulted in almost complete loss of reactivity to the antibody, showing that the COOH terminus is exposed on the lumenal side of the membrane. Removal of the extrinsic polypeptides of the oxygen-evolving complex resulted in an increase of the accessibility of the α subunit to trypsin. These data establish that the α subunit of cytochrome b-559 crosses the membrane once, as predicted from its single, 26-residue, hydrophobic domain. The NH_2 terminus of the α polypeptide is on the stromal side of the membrane, where it is accessible, most likely at Arg-7 or Glu-6/Asp-11, to trypsin or V8 protease, respectively. As a consequence of this orientation, the single histidine residue in the α subunit is located on the stromal side of the hydrophobic domain. Because the β subunit contains a single histidine with a similar location in its hydrophobic domain, heme coordination by an αβ heterodimer would require that both hemes be positioned on the stromal side. (Supported by NIH GM-38323.)

Tu-AM-G2 SITE-DIRECTED MUTAGENESIS INDICATES THAT THE DONOR TO P_{680}^+ IN PHOTOSYSTEM II IS TYR-161 OF THE D1 POLYPEPTIDE
R.J. Debus*, B.A. Barry*#, I. Sithole*, G.T. Babcock#, and L. McIntosh*+, MSU-DOE Plant Research Laboratory*, Depts. of Chemistry#, and Biochemistry+, Michigan State Univ., E. Lansing, MI 48824

Photosystem II contains the two redox-active tyrosines Y_Z and Y_D (1-3). Y_Z transfers electrons from the Mn cluster at the site of water oxidation to the oxidized reaction center primary donor, P_{680}^+. Y_D has an unknown function, but Y_D^+ gives rise to the dark-stable EPR spectrum known as Signal II. We recently established that Y_D is tyr-160 of the D2 polypeptide by site-directed mutagenesis of a psbD gene in the unicellular cyanobacterium Synechocystis 6803 (4). Y_Z is most likely the symmetry-related tyr-161 of the D1 polypeptide (4). To test this hypothesis, we have changed tyr-161 to phenylalanine by site-directed mutagenesis of a psbA gene in Synechocystis. The resulting mutant assembles PSII, as judged by its ability to generate the Y_D^+ radical, but it is unable to grow photosynthetically and exhibits altered fluorescence properties. The nature of the altered fluorescence indicates that forward electron transfer to P_{680}^+ is disrupted in the mutant, as expected for an organism that lacks Y_Z. These results provide strong support for the identification of Y_Z with tyr-161 of the D1 polypeptide.

Work supported by the DOE, NIH, NSF, USDA, and by the McKnight Foundation.

(1) B.A. Barry & G.T. Babcock (1987) Proc. Natl. Acad. Sci. USA 84, 7099-7103.
(2) C.W. Hoganson & G.T. Babcock (1988) Biochemistry 27, 5848-5855.
(3) S. Gerken, K. Brettel, E. Schlodder & H.T. Witt (1988) FEBS Lett. 237, 69-75.
(4) R.J. Debus, B.A. Barry, G.T. Babcock & L. McIntosh (1988) Proc. Natl. Acad. Sci.USA 85,427-430.

Tu-AM-G3 ON THE ELECTROGENIC MECHANISM OF THE CHLOROPLAST CYTOCHROME b_6-f COMPLEX: SEARCH FOR THE Q CYCLE.
P. N. Furbacher, M. E. Girvin, and W. A. Cramer, Department of Biological Sciences, Purdue University, West Lafayette, Indiana, 47907.

The properties of spinach chloroplast cytochrome b_6 have been examined with regard to the role of the b_6-f complex in quinol oxidation and H^+ translocation. The two hemes of the cytochrome, b_p and b_n, on the sides of the membrane with positive and negative $\tilde{\mu}_{H^+}$, have similar spectra (reduced α-band maxima, 563-564 nm, 20°C) and midpoint potentials *in situ* when measured at six different pH values (E_{m7} = -40 mV). Although both hemes are approximately equipotential, and reducible by dithionite in the presence of a redox mediator, only one heme, b_n, was reducible in the dark by NADPH and ferredoxin. The extent of reduction by a flash is 0.6-0.75 heme in the presence of a reduced quinone pool and the inhibitor NQNO. In the presence of NQNO, multiple flashes did not cause an increase in the amplitude of b_6 reduction, as expected if electrons can be transferred from heme b_p to b_n. The amplitude of the flash-induced reduction in the presence and absence of NQNO was not affected by prior reduction by NADPH-ferredoxin, showing that the heme b_p is reduced by the light flash, and that NQNO interacts with heme b_p (blocking oxidation or shifting E_m), but at a site distinct from that of DBMIB-like inhibitors. This is one example where the simple classification of inhibitor, and presumed quinone binding sites, as n and p [or (c and z), (i and o)], may not be sufficient. Thus, one is unable to obtain evidence for reduction of more than one heme associated with PQH_2 oxidation. The two hemes of cytochrome b_6 do not seem to readily communicate, implying that the mechanism of electrogenic H^+ translocation may not involve the interheme electron transport pathway specified by the Q cycle model. (Supported by NIH GM-38323).

Tu-AM-G4 THE EXCHANGE INTERACTION BETWEEN Cu^{2+} AND Q_A^- IN REACTION CENTERS FROM RB. SPHAEROIDES R-26 IN WHICH Fe^{2+} HAS BEEN REPLACED BY Cu^{2+};* R. Calvo, M. Passeggi, INTEC-CONICET, Argentina, R.A. Isaacson, M.Y. Okamura and G. Feher, UCSD, La Jolla, CA 92093.

Exchange interactions provide important information about electron transfer (e.g. see following abstract by Okamura & Feher). We have obtained the exchange interaction between Cu^{2+} and Q_A^- from a comparison of the EPR spectra of $Cu^{2+}Q_A$ and $Cu^{2+}Q_A^-$ in reaction centers (RCs) from Rb. sphaeroides R-26.(1) Unreduced RCs ($Cu^{2+} - Q_A$) gave a typical powder spectrum (see Fig.) having axial symmetry, corresponding to a $d(x^2 - y^2)$ ground state orbital, with $g_{\|} = 2.31$, $g_{\perp} = 2.06$ and with hyperfine interaction parameters $A_{\|} = 155 \times 10^{-4}$ cm^{-1}, $A_{\perp} = 10 \times 10^{-4}$ cm^{-1}. The spectrum changes drastically when the sample is reduced with dithionite ($Cu^{2+} - Q_A^-$) due to the magnetic interactions of the Cu^{2+} and Q_A^- spins. A model spin Hamiltonian proposed for the copper-quinone complex accounted well for the observed spectra. An isotropic exchange coupling of $|J| = 0.36$K was deduced. The anisotropic component of J was an order of magnitude smaller. The isotropic value is similar to that obtained for the Fe^{2+}-Q complex (~0.4K).(2) The exchange interactions will be discussed in terms of the recently determined three-dimensional structure.(3)

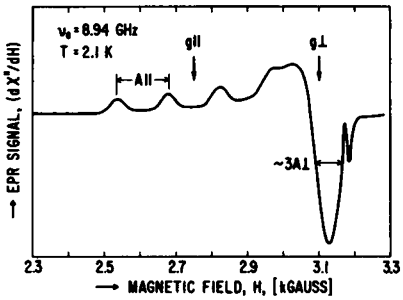

(1)Debus, Feher, Okamura, Biochemistry 25, 2276-2287 (1986). (2)Butler, Calvo, Fredkin, Isaacson, Okamura, Feher, Biophys. J. 45, 947-973 (1984). (3)Allen, Feher, Yeates, Komiya, Rees, Proc. Natl. Acad. Sci. 84, 5730-5734 (1987). *Work supported by the NSF.

Tu-AM-G5 SUPEREXCHANGE MECHANISM OF ELECTRON TRANSFER FROM Q_A^- TO Q_B IN THE Fe-QUINONE COMPLEX OF BACTERIAL REACTION CENTERS;* M. Y. Okamura and G. Feher, UCSD, La Jolla, CA 92093.

A mechanism for electron transfer from the primary quinone Q_A to the secondary quinone Q_B in bacterial RCs is proposed which involves thermally activated electron tunnelling through the intervening Fe-histidine complex by a superexchange mechanism. This mechanism can explain the lack of dependence of the rate on metal substitution(1,2) if a) the reaction is adiabatic, i.e. independent of the electron transfer matrix element or b) the matrix element for electron transfer is only weakly dependent on the nature of the metal ion. The superexchange matrix element for electron transfer is proportional to the exchange coupling J between the metal ion and Q^-. The values of J for $Q_A^-Fe^{2+}$ and $Q_A^-Cu^{2+}$ were found to be very similar (see preceding abstract by Calvo et al). The thermally activated tunnelling mechanism can also explain the experiment by Kleinfeld et al(3) in which electron transfer between Q_A and Q_B occurred at cryogenic temperature when RCs were frozen under illumination but did not occur when RCs were cooled in the dark. These results can be explained if the configuration of the RCs cooled in the light, i.e. in the product state $Q_AFe^{2+}Q_B^-$, closely resembles that of the transition state.

(1)H.K. Nam, R.H. Austin and G.C. Dismukes (1984) Biochim. Biophys. Acta, 765, 301. (2)R.J. Debus, G. Feher and M.Y. Okamura (1986) Biochemistry 25, 2276. (3)D. Kleinfeld, M.Y. Okamura and G. Feher (1984) Biochemistry 23, 5780. *Work supported by the NSF.

Tu-AM-G6 pH DEPENDENCE OF THE FREE ENERGY GAP BETWEEN DQ_A AND $D^+Q_A^-$ DETERMINED FROM THE DELAYED FLUORESCENCE OF $D^+Q_A^-$ IN RCS FROM RB. SPHAEROIDES R-26;† P.H. McPherson, M.Y. Okamura and G. Feher, UCSD, La Jolla, CA, and V. Nagarajan and W.W. Parson, University of Washington, Seattle.

The free energy gap between DQ_A and DQ_A^- determined from redox titrations of isolated RCs(1) increases between pH 6 and 10 approx. 2-3 fold more than predicted from the proton uptake of DQ_A^-(1,2). To investigate the cause of this discrepancy, we have used an independent method (delayed fluorescence) to determine the pH-dependence of a related free energy gap: ΔG_1^o, between DQ_A and $D^+Q_A^-$ (see inset in Fig.). The pH-dependence of ΔG_1^o (dots in Fig.) was determined from the delayed fluorescence amplitude F_d using the relation: $F_d = k_f \cdot [D^*Q_A] = k_f \cdot [D^+Q_A^-] \cdot \exp\{-(\Delta G_2^o - \Delta G_1^o)/kT\}$, where k_f is the radiative rate constant and ΔG_2^o is the energy of the optically excited state. Corrections due to the pH-dependence of k_f and ΔG_2^o were estimated from the integral of the absorption spectrum (dimer band) using the Strickler-Berg relation and the position of the absorption maximum, respectively (k_f and ΔG_2^o decreased ~6% and ~7 meV, respectively, from pH 6.5 to 7.5 and were ~pH-independenct at pH > 7.5). ΔG_1^o obtained by integrating the proton uptake of $D^+Q_A^-$(2) (solid line in Fig.) is in satisfactory agreement with the delayed fluorescence results. This agreement validates the method used to measure proton uptake, and suggests a reexamination of the redox titration results. (1)P. Maróti and C.A. Wraight (1988) BBA 934, 329-347. (2)P.H. McPherson, M.Y. Okamura and G. Feher (1988) BBA 934, 348-368. †Work supported by NSF.

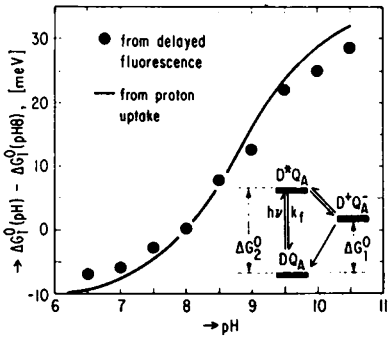

Tu-AM-G7 EPR AND ENDOR STUDIES OF $D^+Q_AFe^{2+}Q_B^-$ IN SINGLE CRYSTALS OF RCs FROM RB. SPHAEROIDES;* J.P. Allen, E.J. Lous, R.A. Isaacson, M.Y. Okamura and G. Feher, UCSD, La Jolla, CA 92093.

The primary and secondary acceptors in bacterial photosynthesis are quinones (UQ-10), which in their reduced states couple magnetically to a high spin Fe^{2+}. The electronic state of the ferroquinone complexes had been probed by low temperature EPR solution studies[1]. The spectra were explained by invoking the 2 lowest magnetic states of the iron manifold and by attributing the large linewidth (~10^3 Gauss) to the g-anisotropy of the Fe^{2+}. To refine this model and to correlate the parameters with the three-dimensional structure, we obtained EPR spectra on single crystals of RCs (space group $P2_12_12_1$) whose structure has been determined by X-ray diffraction.[2] RCs were frozen under illumination to produce the stable charge separated state $D^+Q_AFe^{2+}Q_B^-$. The spectrum, with H perpendicular to the c-axis of the crystal, shows 2 well resolved lines at g≃1.8 and g≃1.9 (see Figure) due to the interaction of Q_B^- with the Fe^{2+}. The lines shift and broaden as the magnetic field is rotated about the c-axis. The line at g≃2.003 is predominantly due to D^+ (overmodulated and saturated). We have also obtained ENDOR spectra of D^+ from single crystals; these studies allow the determination of the anisotropic components of the hyperfine interactions. [1]Butler, Calvo, Fredkin, Isaacson, Okamura and Feher; Biophys. J. 45, 947-973 (1984). [2]Allen, Feher, Yeates, Komiya and Rees, PNAS 84, 5730-5734 (1987). *Work supported by the NIH, NSF and EMBO.

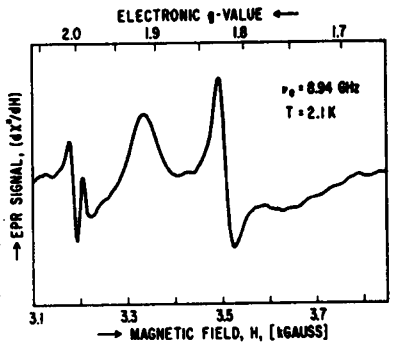

Tu-AM-G8 ACCESSORY BACTERIOCHLOROPHYLL IS REQUIRED FOR TRIPLET ENERGY TRANSFER BETWEEN THE PRIMARY DONOR AND THE CAROTENOID IN PHOTOSYNTHETIC BACTERIAL REACTION CENTERS. Harry A. Frank, Kristin Conneli and Carol A. Violette, Department of Chemistry, University of Connecticut, Storrs, Connecticut, 06269-3060, USA.

Reaction centers from the carotenoidless mutant *Rb. sphaeroides* R26 were treated with sodium borohydride which is known to remove the accessory monomeric bacteriochlorophyll (Bchl) bound to the M protein subunit [1]. Afterwards, the carotenoid, spheroidene, was incorporated into the modified reaction centers. It is demonstrated by optical absorption, circular dichroism and electron spin resonance spectroscopy that spheroidene reconstituted into the borohydride-treated *Rb. sphaeroides* R26 reaction centers is bound in a single site, in the same environment and with the same structure as spheroidene reconstituted into untreated *Rb. sphaeroides* R26 reaction centers. Furthermore, the data indicate that unless the accessory Bchl is present, the primary donor-to-carotenoid triplet energy transfer reaction is inhibited. These observations provide direct evidence for the involvement of the accessory Bchl in the triplet energy transfer pathway. This was suggested by the X-ray crystal structure of the carotenoid-containing *Rb. sphaeroides* wild type 2.4.1 which showed that the accessory Bchl was located between the primary donor and the carotenoid [2]. In a different set of experiments carried out on the *Rb. sphaeroides* 2.4.1 reaction center, it was found that borohydride removes *both* the accessory Bchl *and* spheroidene from the protein and inhibits the triplet energy transfer reaction. This work is supported by grants from the USDA (88-37130-3938) and NIH (GM-30353).

1. P. Maroti, C. Kirmaier, C. Wraight, D. Holten and R. M. Pearlstein (1985) Biochim. Biophys. Acta **810**, 132-139.
2. J. P. Allen, G. Feher, T. O. Yeates, H. Komiya and D. C. Rees (1988) In *The Photosynthetic Bacterial Reaction Center*, J. Breton and A. Vérméglio, eds., Plenum Press, New York, pp. 5-12.

Tu-AM-G9 DETERMINATION OF THE PRIMARY CHARGE SEPARATION RATE IN ISOLATED PHOTOSYSTEM II REACTION CENTERS WITH 500 FEMTOSECOND TIME RESOLUTION

M. R. Wasielewski*, D. G. Johnson*, M. Seibert‡, and Govindjee§
*Chemistry Division, Argonne National Laboratory, Argonne, IL 60439; ‡Photoconversion Research Branch, Solar Energy Research Institute, Golden, CO 80401; §Departments of Physiology and Biophysics, and Plant Biology, University of Illinois, Urbana, IL 61801

We have measured directly the rate of formation of the oxidized chlorophyll a electron donor ($P680^+$) and the reduced electron acceptor pheophytin a^- (Pheo a^-) following excitation of isolated Photosystem II reaction centers (PS II RC) at 4 °C. The RC complex consists of D_1, D_2, and cytochrome b-559 proteins and was prepared by a procedure which stabilizes the protein complex. Transient absorption difference spectra were measured from 440 - 850 nm as a function of time with 500 fs resolution following 610 nm laser excitation. The formation of $P680^+$ - Pheo a^- is indicated by the appearance of a band due to $P680^+$ at 820 nm and corresponding absorbance changes at 505 and 540 nm due to formation of Pheo a^-. The appearance of the 820 nm band is monoexponential with $\tau = 3.0 \pm 0.6$ ps. The decay of the lowest excited singlet state of P680 can be monitored at 650 nm. The time constant for decay of this state is $\tau = 2.6 \pm 0.6$ ps and agrees with that of the appearance of $P680^+$ within experimental error. Thus, primary charge separation in PS II occurs with a time constant very similar to that observed in the purple photosynthetic bacteria, Rb. sphaeroides and Rps. viridis. Treatment of the PS II RC with sodium dithionite and methyl viologen followed by exposure to laser excitation, conditions known to result in accumulation of Pheo a^-, results in formation of a transient absorption spectrum due to the lowest excited singlet state of P680. Under these conditions charge separation does not occur. We find no evidence for an electron acceptor that precedes the formation of Pheo a^-. We have also obtained results at 15K which will be reported.

Work at ANL was supported by the U.S. Department of Energy, Office of Basic Energy Sciences, Division of Chemical Sciences under contract W-31-109-Eng-38. Work at SERI was supported by the Energy Biosciences Division, Office of Basic Energy Sciences of the U.S. Department of Energy under contract 18-006-88 and by the SERI Director's Development Fund.

Tu-AM-G10 **Electronic States of Isolated and Reaction-Center Bound Carotenoides.**

Chian-Fan Zhang*, Carol A. Violette+, Harry A. Frank+ and Robert R. Birge*
* Department of Chemistry, Syracuse University, Syracuse, NY 13244
+ Department of Chemistry, University of Connecticut, Storrs, CT 06269

INDO-PSDCI calculations on the optical absorption properties of spheroidene isomers in solution as well as bound in the reaction center of *Rhodobacter Sphaeroides 2.4.1* have been carried out. For spheroidene with an all-trans or 15-cis planar geometry, the calculated peak positions and the relative absorptivities of the allowed excited states are found to be in good agreement with the observed absorption spectra. We conclude that INDO-PSDCI procedures are reliable for predicting the properties of the allowed excited states of spheroidene. INDO-PSDCI calculations on the X-ray geometry of spheroidene in the reaction center [1], however, predict allowed electronic transitions which do not coincide with experimental observation. Furthermore, the calculated ground state energy of the X-ray structure is 103 kcal/mole higher than the planar all-trans conformation. The calculation predicts that the 15-cis geometry is 3.8 kcal/mole higher in energy than the energy calculated for the all-trans species. These results suggest that the primitive X-ray geometry of spheroidene in the bacterial reaction center requires further refinement. We thank Drs. Rees and Feher for kindly providing us the X-ray coordinates of spheroidene in the bacterial reaction center.

1. J.P. Allen, G. Feher, T.O. Yeates, H. Komiya and D.C. Rees (1988) in *Photosynthetic Bacterial Reaction Centers*, J. Breton and A. Vermeglio, eds., Plenum Press, NY, pp. 5-12.

Tu-AM-G11 ASSESSMENT OF ACID-DAMAGE TO PHOTOSYNTHESIS BY PHOTOACOUSTIC SPECTROSCOPY.

N'soukpoé-Kossi, C.N., S. Keilani, H. Proteau, R. Bélanger and R.M. Leblanc, Université du Québec à Trois-Rivières, Centre de recherche en photobiophysique, C.P. 500, Trois-Rivières, Québec, Canada, G9A 5H7.

The impact of air pollution on plants has become one the most important subject in plant sciences nowadays. Because of its socio-economical and political implications, it spurts a flood of controversies about the actual causative factors, among which acid precipitations along with O_3 and SO_2 play a pivotal role. The common assays used to diagnose forest decline remain visual and most of the time, subjective and rather late. We have used photoacoustic spectroscopy (PAS) to assess the acid-damage to photosynthesis by monitoring O_2-evolution in leaves from corn and sugar maple plantlets in a growing chamber. The seedlings have been treated with simulated acid rains either by flushing the leaves or by watering the soil for 2 months. The results indicate a linear-like decline of O_2-evolution as the pH of pulverization decreases. As for plantlets treated by watering the soil with acid mixture, the results are not yet conclusive, although some tendency towards low photosynthetic activity is observed for maple leaves. The reduced photosynthetic activity is sometimes accompanied by depigmentation and death (below pH:3.5). Corn seedlings from seeds which have germinated in acid media, present special features: low rate of germination at low pH; higher initial rate of growth at low pH than at higher pH, and high rate of mortality at low pH values. The surviving seedlings all show similar O_2-evolution rate by PAS. These results clearly indicate the importance of acid-damage to photosynthesis at foliar level and the ability of PAS to assess precociously the forest decline.

Tu-AM-G12 THE STARK EFFECT IN ANTENNA PROTEINS FROM RB. SPHAEROIDES;*

M. Loesche, Johannes-Gutenberg Universität, D6500 Mainz, West Germany, and P.B. Madden, G. Feher and M.Y. Okamura, University of California, San Diego, La Jolla, CA 92093.

Stark Effect measurements[1,2] have been made on the antenna proteins from the photosynthetic bacterium *Rhodobacter spheraoides* at 77K. The B-800-850 species purified with β octyl-glucoside shows a Stark spectrum (Fig. c) with a lineshape proportional to the second derivative of the absorption spectrum (Fig b) resulting from a change in dipole moment $\Delta\mu$, between the ground and excited states. The long wavelength 849 nm band shows a much larger Stark effect ($\Delta\mu$= 3.3 Debye, δ=46°) than the band at 797 nm (($\Delta\mu\simeq$1 Debye)). The B870 species (in chromatophore membranes) gave a large Stark effect ($\Delta\mu\simeq$6 Debye) at 877 nm similar to that of the primary donor special Bchl pair in Rb. sphaeroides[1,2]. The larger values for $\Delta\mu$ found for the long wavelength antenna bands are consistent with a dimeric structure[3] and suggest that the shift to longer wavelengths results from mixing of charge transfer states.[4]

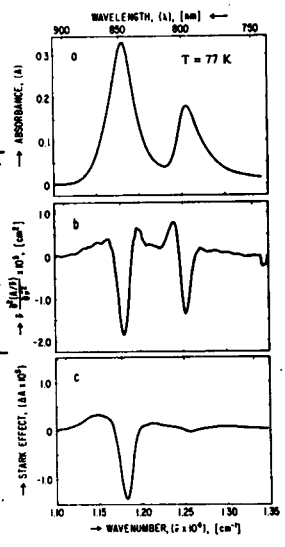

[1] D.J. Lockhart and S.G. Boxer (1987) Biochemistry 26, 664. [2] M. Loesche, G. Feher and M.Y. Okamura (1987) Proc. Natl. Acad. Sci. USA 84, 7537.
[3] Kramer, Van Grondell, Hunter, Westerhaus and Amesz, Biochim. Biophys. Acta 765 (1984). [4] W.W. Parson and A. Warshel (1987) J. Am. Chem. Soc. 109, 6152.

*Work supported by the NSF and FDG.